REVIEW ARTICLE

Aydan GARROD, Aritra GHOSH

A review of bifacial solar photovoltaic applications

Abstract   Bifacial photovoltaics (BPVs) are a promising alternative to conventional monofacial photovoltaics given their ability to exploit solar irradiance from both the front and rear sides of the panel, allowing for a higher amount of energy production per unit area. The BPV industry is still emerging, and there is much work to be done until it is a fully mature technology. There are a limited number of reviews of the BPV technology, and the reviews focus on different aspects of BPV. This review comprises an extensive in-depth look at BPV applications throughout all the current major applications, identifying studies conducted for each of the applications, and their outcomes, focusing on optimization for BPV systems under different applications, comparing levelized cost of electricity, integrating the use of BPV with existing systems such as green roofs, information on irradiance and electrical modeling, as well as providing future scope for research to improve the technology and help the industry.

Keywords   bifacial photovoltaics (BPVs), bifacial, photovoltaics, applications, review, solar

1   Introduction

For all countries, the most important challenge they face today is to ensure sustainability while struggling with environmental degradation [1], due to the carbon dioxide emitted by non-renewable energy sources [2–4]. Countries must do this while keeping a balance of not only energy sustainability but also allowing energy security, as well as maintaining equitable access to energy, also known as the energy trilemma [5]. Renewable electricity generation stands at an all-time high of 30% as of 2021, with further advances expected

Aydan GARROD, Aritra GHOSH (✉)
Faculty of Environment, Science and Economy (ESE), Renewable Energy, Electric and Electronic Engineering, University of Exeter, Penryn TR10 9FE, UK
E-mail: a.ghosh@exeter.ac.uk

of 50% by 2030, and 80% by 2050 [6,7]. Investment in green energy is crucial [8] to decrease the use of fossil fuel-based energy sources and greenhouse gas emissions [9,10], levels of which 2010–2019 were higher than at any previous decade recorded [11]. The recognition of this issue put into practice can be seen in a number of examples, such as the creation of sustainable development goal which has the goal of ensuring access to affordable, reliable, sustainable, and modern energy for all [12–14]. The development of this goal can be seen in Liu et al. [15] through the adoption of renewable energy technologies in the G7 countries, it is also of course noticeable though, that the trend is improving year on year. Though it is of course simpler for wealthier nations to transition toward net zero than less developed, or wealthy nations as developing countries are still needing to question whether sustainable human development should be achieved at the price of economic growth [16] as shown in Sueyoshi et al. [17]. The issue is also dealt with in the decision to limit global warming to 1.5 °C [18].

As a result of the recognition of the need for renewable energy sources to reduce the greenhouse gases (GHGs) produced by fossil fuels, many countries have been increasing the contribution that renewables make to their energy supply [8]. While doing this, it is important to ensure that the transition to renewables remains affordable, especially in the case of developing regions to avoid the adoption of low-cost fossil fuel-based energy sources known as the "curse of development" [19,20]. The levelized cost of electricity (LCOE) of solar energy is lower than offshore wind, but still more expensive than onshore wind and hydropower [21]. However, in the coming years, solar energy is expected to become less expensive than wind energy [22], making it an ideal method of renewable energy to focus on for the future.

Solar photovoltaics (PVs) systems have gone through many different iterations, the first cell being made of selenium in 1883 [23]. The first generation of panels were made of monocrystalline or polycrystalline silicon with conversion efficiencies of 26.8% ± 0.4% [24] and 15% [25], respectively. The second generation are made

of amorphous silicon (a-Si) conversion efficiency of 10.3% [24], cadmium telluride (CdTe) conversion efficiency of 21% [24], and copper indium gallium selenide (CIGS) conversion efficiency of 19.95%–21% [26]. The third and most recent generation includes dye-sensitized solar cells (DSSCs) having a conversion efficiency of 11.9% [24], a perovskite conversion efficiency of 25.7% [27], and organic with a conversion efficiency of up to 11% [28]. The energy density of solar energy is currently lower than that of conventional fossil fuel energy sources [29]. One way in which solar panels can have a higher energy density is through the use of bifacial panels, which will be the focus of this paper. Bifacial panels are able to produce more electricity than their monofacial counterparts due to the fact that they are able to utilize incident irradiance on both the front and rear sides of the panel [30]. This is demonstrated in Figs. 1 and 2.

This review will provide an up-to-date examination of bifacial PV technologies across the most common applications. Due to the length of time since the last publication in this area, and the fast-evolving nature of this technology, a new technology review is much needed. The previous bifacial photovoltaic (BPV) technology review [31] focuses on types of bifacial cells and modules. Unlike the review of Guerrero-Lemus et al. [31], this review focuses on the various applications of BPV panels, such as agrivoltaics, building mounted, and ground mounted etc. and their optimization to maximize the energy generation from the system. Other previous technologies analyzing BPV technologies can be seen in Table 1.

As seen above in Table 1, all BPV review papers have brought a novelty to the industry not previously investigated thoroughly. Many past review papers have looked more at small module-level technology aspects such as cell degradation or improving module electrical performance. As far as applications are concerned, Ref. [36] has reviewed agrivoltaic and aquavoltaic applications, referred to as floating PV in this paper. However, not only are these only two of multiple applications of photovoltaics, they are also two of the more niche applications involving photovoltaics. BPV is expected to become a dominant force in the PV industry in the coming years. Therefore, it is necessary for the industry to be presented with a review encompassing all major applications of BPV to ensure that the current scope on research in the topic is documented collating results and knowledge gathered to this point and suggesting topics for research in the future to further the industry.
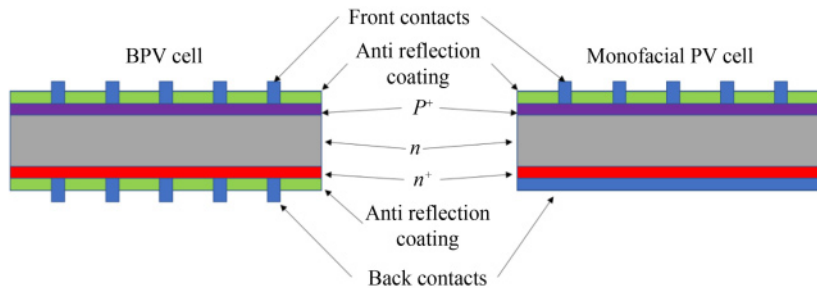

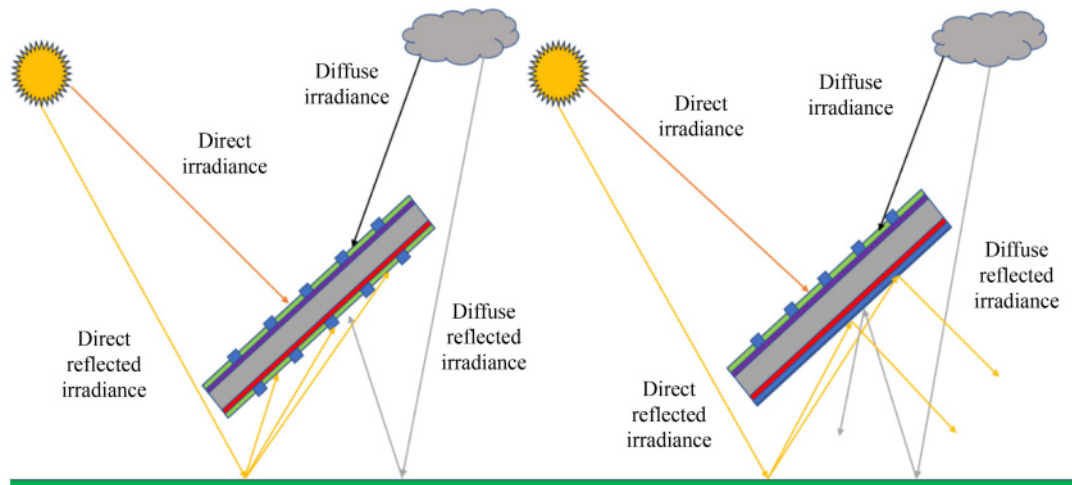**Fig. 1**   Comparison of the cell structure of monofacial and BPV cells.

Fig. 2   Example of the difference in the working principle of bifacial and monofacial PV panels.

Table 1 Novelties of past and present BPV review papers

Ref.	Novelty
Gu et al. [32]	Outlooks for different aspects of the BPV technology
Guerrero-Lemus et al. [31]	First major review of the BPV technology
Lorenzo [33]	Origins of BPV modeling
Raina & Sinha [34]	Provides future novel concepts for improved performance and reliability of bifacial modules, as well as potential applications of the BPV technology
de Bastiani et al. [35]	Origins of BPV and its development
Mouhib et al. [36]	Agrivoltaic and aquavoltaic BPV applications
Molto et al. [37]	Potential-indued degradation of BPV modules
Current review	In-depth examination of bifacial applications and scope for optimization and further research topics

2 BPV

The first commercialized BPV modules were developed by ISOFOTON, a Spanish academic spinoff founded in 1981. Many initiatives were developed in order to increase the output power and among these were three bifacial cells produced in 1979 with different structures. A transcell with an n^+pn^+ structure, vertical multijunction cell made up of a pile of n^+pp^+ wafers, and a double-sided back surface field cell with a p^+nn^+ structure [38]. The chosen structure was the double-sided back surface field cell with a p^+nn^+ structure, i.e., a passivated emitter rear totally diffused (n-PERT) cell, which at that time had a proven efficiency of 12.7% with back illumination [38]. Figure 3 is an example of some of the original BPV modules.

In 1980, it was found that BPV panels could produce between 42% and 63% more output power than a conventional panel [39]. The first five bifacial panels came out in early 1983, with 10, 22, 35, 45, and 90 Wp, with the rating taken from solar irradiance levels of 1000 and 500 W/m^2 for the front and rear sides of the panel respectively [38]. Figure 2 demonstrates the difference between more traditional monofacial PV cell structure and BPV cell structure, showing the ability of bifacial cells to utilize incident as well as albedo light.

The popularity and interest of BPV have clearly grown over time, especially in the last couple of decades, (see the increase of BPV in the market share of PV in Fig. 4, which was around 15% back in 2019), and the market share was predicted to jump by 100% to 30% by 2022, which it has done, shown when stated in Eguren et al. [38] that BPV modules represent over 30% of new installed capacity. Meaning that the predicted trends of this study are true thus far, meaning that by 2030 in 7 years' time it is likely that the market shares of monofacial and BPV will have reversed, as BPV will represent 70% of the PV market.

The trend is similar when looking at the number of papers published covering the BPV technology over time in Fig. 5, in which a steady incline can be seen up until the late 2010s, at which point a much larger increase in

Fig. 3 Examples of the first BPV modules (adapted with permission from Ref. [38]).

the number of papers being published on the subject can be seen. The 2023 figures are for papers released up until August of that year. This figure shows a definite rise to prominence in the industry of photovoltaics for bifacial technologies.

3 BPV for various applications

This section will analyze different applications of BPV systems while identifying different factors that make the BPV system more or less effective. It will analyze the advantages and disadvantages of swapping conventional monofacial PV for BPV, why it is more effective and by how much. It will also identify when the benefits of installing BPV are nullified and not deemed worthy of the extra cost currently incurred in making the swap. Ground-mounted systems are the most widely used for large-scale commercial solar farms, and power generation of these commercial sites can be greatly increased through the inclusion of BPV panels. The other possible applications for the BPV technology can be floating, building integrated photovoltaics (BIPVs), and building applied photovoltaics (BAPVs) and agrivoltaics as shown in Fig. 6.
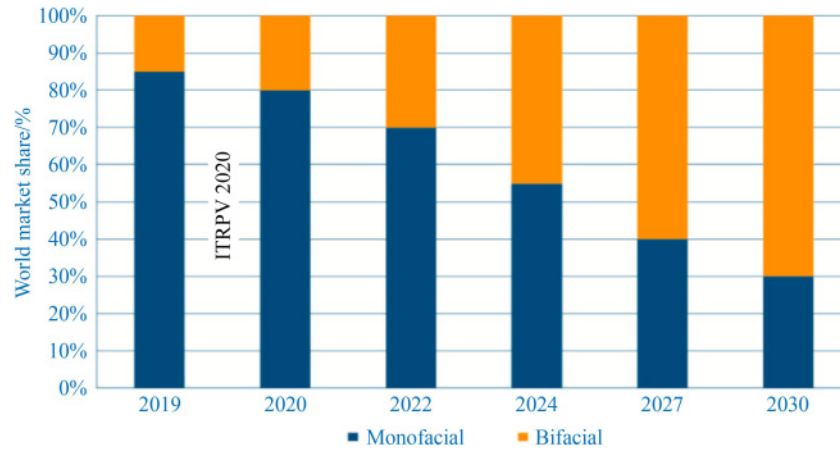
Fig. 4 Comparison of the predicted market share of monofacial and BPV over time (adapted with permission from Ref. [32]).
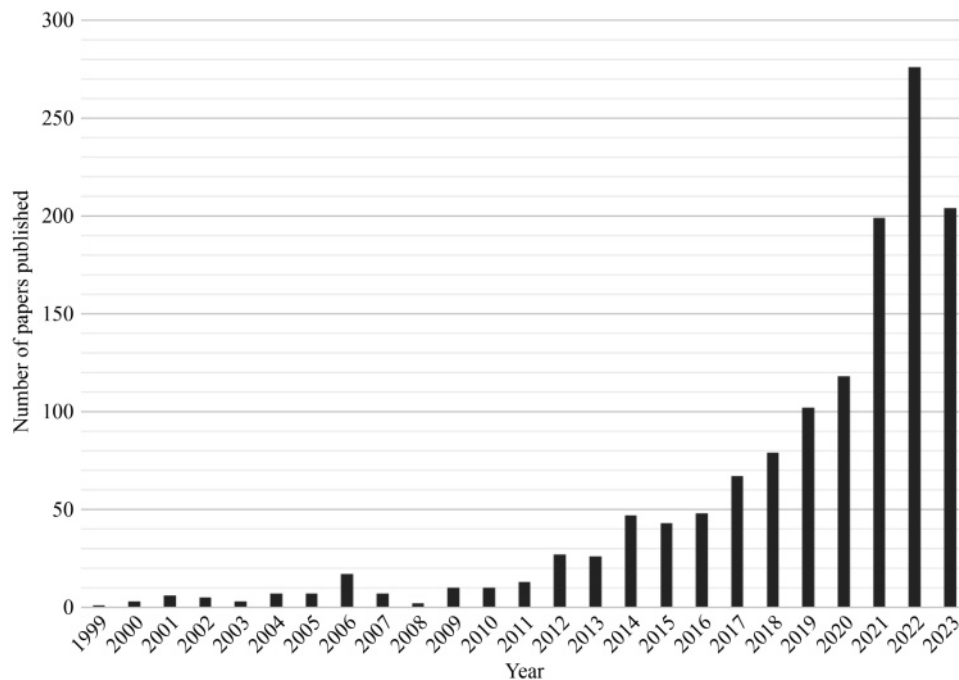

Fig. 5 Number of papers published on BPV from 1999 to 2023 (source: ScienceDirect).

3.1 BPV for ground-based PV

3.1.1 BPV for ground-mounted PV

As stated earlier, BPV panels can add an extra 42%–63% to the power output compared to a conventional panel [39], when applied in a real-world situation with a ground-mounted panel. A BPV system can offer 25%–30% additional power output when installed in an optimized configuration [40]. The level of solar irradiance incident on the solar cell, along with cell temperature, is one of the main factors that affects the power output of a cell. With BPV, the shading aspect for the front side of the panel are not just concerned with, as

would be with a monofacial panel. Crucially, the irradiance on the rear side of the panel must also be considered, taking into consideration the height of the panel off the ground, the panel's angle of tilt, and the albedo of the surface the panel is mounted on. The higher the albedo, the more irradiance is reflected off the surface onto the panel.

To maximize the benefit of the BPV panel, the albedo must be as high as possible. There are various ways to achieve this. Muehleisen et al. [41] conducted a study in which the energy yield of a BPV system was compared to that of a monofacial PV system. To do this, they used three different module configurations, comparing the gain due to bifacial solar cells, as well as a comparison with a
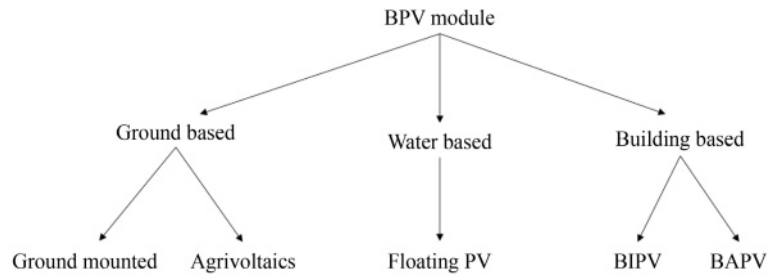
Fig. 6   A breakdown of BPV applications.

lower and a higher bifaciality factor. The bifaciality factor is the nominal efficiency at the rear side of the panel, compared with the nominal efficiency at the front side of the panel. To create a higher albedo, the concrete surface the panels were installed on was painted white. The minimum ground clearance of the panels was 40 cm, whereas conventional design setups was only 5 cm. Modules were orientated in both east and westerly directions. The results of this study concluded that the average benefit of the BPV technology is 17% for east facing modules, and 15% for west facing modules when compared with monofacial modules facing the same direction. However, the gain reduced to 7% and 5% for east and west respectively after one year of operation. The reason for this seems to be due to the moss growth and dust on the white surface, indicating that in order to get a worthwhile benefit from BPV modules, it is not just the panel itself that must be optimized, but the surroundings as well. Muehleisen et al. [41] looked at a more conventional ground-mounted layout for a PV system, in which there was a front and rear side, where one side of the panel faced toward the ground. Khan et al. [42] looked at a setup which was more unique to suit a BPV panel, where the panels were mounted vertically. While this design is not used for monofacial panels, there are a number of reasons why it is beneficial for the use of BPV. One aspect to consider when looking at the use of vertically mounted modules is the generation profile, as this differs dramatically when compared to a conventionally mounted monofacial module.

This is demonstrated in Fig. 7, in which it can be seen that a vertically mounted BPV module facing east–west orientation produces more energy in the morning and late afternoon than conventionally mounted monofacial modules. This type of production profile is interesting, as unlike monofacial modules, it shows that bifacial modules are able to fit the traditional demand curve or "duck curve" explained in Hou's study [44]. Figure 7 was created from a simulation in Singapore. It should, therefore, be noted that for locations of significantly higher latitude, the generation profile could differ dramatically between summer and winter months due to a lower zenith angle in the winter months. In the study by Guo et al. [43], which was very general and did not
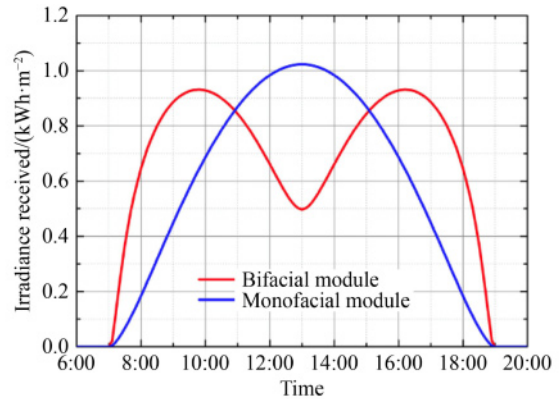

Fig. 7   An example of the received irradiance profile of a vertically mounted BPV module compared to a monofacial module (adapted with permission from Ref. [43]).

consider different panel types, the vertically mounted BPV modules received only 1% more radiation than monofacial modules. However, this study was simulated with an albedo value of 0.2, which was low, whereas Ref. [41] which concluded a much higher benefit from BPV modules actively, improved the albedo of the ground through white paint.

A more detailed study was conducted for vertical bifacial solar farms in Ref. [42], which took an albedo level of 0.5. It compared vertically mounted BPV panels to optimally mounted monofacial PV panels, and concluded that in almost all regions of the world, vertically mounted BPV panels were able to outperform the monofacial panels by 10%–20%. In some regions in Africa and South America, the BPV panels were able to offer an energy output 50% higher than that of the monofacial panels. There were locations such as China, Colombia, and Ecuador where the monofacial panels outperformed the BPV panels. However, these locations were characterized by a low clearness index which would mean more shading of the diffuse light at the bottom of the panel [42].

Patel et al. [45] mentioned that panel-to-panel and panel-to-ground shading effects might nullify the perceived advantages of stand-alone BPV farms. Appelbaum [46] looked at the effects of shading. The BPV panels were arranged in multiple rows facing both

east to west and north to south. It was found that BPV panels installed at an optimum tilt angle facing south, the location of the study being Tel Aviv, might, on average, produce 32% more energy than vertical BPV panels facing east–west [46]. It is also worth noting that this study finds that when the angle of a BPV panel to the ground is low (around 20°) that the incident irradiation on the rear side of the panel is negligible [42]. In another study, Khan et al. [47] explored a more novel approach of ground sculpting, in order to achieve a higher albedo and bifacial gain. They concluded that at high degrees of latitude (around 60°), BPV panels with ground sculpting could have a 100% energy gain when compared to a monofacial farm.

Temperature can have a great effect on the efficiency of PV panels. After solar irradiance, it is the most significant factor affecting energy production [48]. BPV modules, however, are able to produce more energy at higher cell temperatures compared to monofacial PV cells [49]. It is, therefore, expected that BPV cells will perform better in the future as climate change affects levels of solar insolation, and the energy yield is expected to drop from 8% to 8.4% between 2020 and 2080 [50]. This bodes well for the future of BPV in hot climates such as Oman where a 105 MWp solar project has been commissioned [49]. As well as the naturally better performance at higher temperatures, work has been done to improve the cooling of bifacial modules to further improve their performance, such as Li et al. [51] who studied cooling fins to improve air cooling methods. A 4.4% power conversion efficiency was recorded under specific circumstances, providing a maximum temperature decrease of 13.6 K. As well as this, Xia et al. [52] altered the glass surface of the panel to allow for better passive cooling methods. Other methods include examples from Ma's study [53] which considered more basic cooling methods, or Gao's study [54] which integrated a heat sink into the panel.

3.1.2   BPV for agrivoltaics/agriphotovoltaics (APVs)

One aspect of photovoltaics which has yet to be mentioned is APV, an example of which can be seen in Fig. 8. In a world with a consistent demand for energy and food, it is essential to develop interrelationships between the food and energy sectors, APV show promising potential for this [55]. APV can provide economic advantages over conventional agriculture and PV systems per unit area [56,57], as well as contributing to United Nations (UNs) sustainable development goal 2 of zero hunger [58]. PV panels mounted over vegetation are able to present lower surface temperatures compared to panels mounted over normal ground [59].

In a study by Williams et al. [61], it was found that an APV system mounted 4 m above soybean crops saw a reduction of panel surface temperature of up to 10 °C

Fig. 8   Vertically mounted bifacial APV system in Sweden (adapted from Ref. [60] under the terms of CC BY license).

increasing energy production, as well as an increased panel lifetime [61]. Because of the nature of APV BPV modules being significantly elevated off of the ground, rear irradiance homogeneity is enhanced, omitting one of the main limiting factors in BPV performance [62]. The albedo level varies with morphological and optical properties for any PV system [63]. However, as an added variation for APV-based BPV, the albedo is crop specific [64], meaning that some crops are more suited to BPV optimization than others. Though it is not just the type of crop that affects the albedo, it is the combination of the albedos of the vegetation and the soil [64,65].

With the integration of PV arrays, microclimate alterations can be anticipated that can directly affect the photosynthetic rate of the crops and their biomass production [66]. Though Marrou et al. [67] concluded that only a few changes were required to switch from open crops for APV, and that instead it was better to focus on mitigating light reduction and utilizing crops that are adaptable. One microclimate adaptation experienced was a reduction in soil temperature due to the shade casted by the PV panels, which led to a decrease in soil evaporation, and an increase in crop yield for maize [68].

In terms of BPV optimization in APV systems, Deline et al. [69] found a logarithmic relationship between panel elevation and rear irradiance, showing that as elevation increased, rear irradiance increased, accompanied with a decrease in spatial non-uniformity. When considering vertically mounted east–west facing BPV panels, when compared to monofacial panels facing north–south, at a pitch angle of 20° for a high to standard level of panel density, both energy yield and crop yield are greater for vertical BPV than monofacial PV, with the gain decreasing as panel density decreases [70].

3.2   BPV for buildings

PV systems can be included in a building in two ways, one being BAPV, and the other being BIPV. These are the two main methods of combining PV technology with buildings [71]. BAPV has no effect on the structural performance of the building [72,73], whereas BIPV is defined by the international standards organization as both a PV and conventional building material [74,75].

3.2.1   BPV- based BAPV

"The building attached/applied photovoltaic (BAPV) does not replace the construction component, can be rack-mounted or standoff arrays type, opaque in nature and are only employed for power generation and do not contribute to any heat gain into the building interior, rather it alleviates heat gain by generating shading the roof or wall from direct solar heat" [76,77]. BAPV systems are already widely applied for small-scale domestic generation on household roofs having benefitted from support schemes such as feed-in tariffs. However, these applications have for the most part involved monofacial panels with little BPV examples to date.

A potential application for bifacial systems is on green roofs. Green roofs are widely used due to their energy saving potential, air pollution reduction, and urban heat island effect reduction in urban contexts [78]. BPV modules that are mounted vertically may be able to provide space for plants and their upkeep, as well as having a PV system that gives specific energy yields comparable to standard flat roof systems [79].

Figure 9 shows an example of the vertically mounted BPV systems on a green roof mentioned in Ref. [79]. This setup concluded that a low ground cover ratio of the panels was required to avoid mutual shading between the panels. This means that the total available capacity to install in kWp per unit area of the roof is smaller than what would be capable if standard monofacial panels were to be used, which means that if the only goal is to maximize the power obtained from the PV system, it would be more advantageous to use a standard monofacial system than a vertically mounted bifacial system. However, if the goal is to maximize the benefits of a green roof and use the BPV system, it is advantageous to have the vertically mounted BPV panels, as it optimizes the space available for taking care of the green roof. For conventional roofs, the bifacial panel is

Fig. 9   Example of a vertically mounted BPV system on a green roof in Winterthur, Switzerland (adapted with permission from Ref. [79]).

not as much of an option, as while it is possible to mount the panels vertically on a slanted roof, there is no evidence of this being done.

There is not much other evidence of BPV being used for BAPV applications other than for roof applications mentioned earlier. This is somewhat surprising, as BPV panels can be adopted in place of monofacial panels, reducing the incurred limitation common with monofacial panels at little additional cost [80,81]. This means that there could be a straight swap between monofacial panels and BPV panels at a little extra cost, without incurring extra cost through optimisation efforts, and it would still be possible to get an advantage from the BPV panels.

As a general statement for the use of BPV applied on buildings, it is worth noting that the reflectance of different materials on which panels could find themselves using the albedo of if mounted on a roof. Different roof materials such as slate, tiles, and corrugated metal have different albedo values. The albedo of these surfaces can be coated with highly reflective substances, as done in Bretz & Akbari [82] in which the albedos of the roof were altered and it was found that by increasing the albedo through using various white coatings, it is also possible to increase the cooling energy savings. In Ramamurthy et al. [83], it is found that a white roof can not only increase albedo and therefore the bifacial gain, but also decrease the cooling load of a building during the summer months, and help mitigate urban heat islands, which will in turn help increase cell efficiency through a decreased cell temperature [84,85]. The roof must be kept clean, however, in order to maximize the albedo and energy generation. If algae, or moss grew on the roof, the ability of the surface to reflect the maximum amount of light would be inhibited and it would be impossible to produce the maximum amount of energy possible, much like bird droppings on the face of a monofacial panel [86].

3.2.2   BPV-based BIPV

According to the International Energy Agency, more than 30% of the world's energy consumption is consumed by buildings [87]. It should therefore be an incentive to either reduce the consumption coming from buildings or ensure a method of renewable energy generation for buildings to avoid excess carbon emissions [88,89]. "Building integrated photovoltaics (BIPVs) have good development prospects, because of its ability to be widely used on the building surface and convert solar energy into electricity" [90]. Although BPV applications on buildings have advantages, it is a novel application of the technology and therefore there is not much research into the application [91]. There are many ways to integrate PV panels into a building, such as for shading purposes [92,93], for roofing [94,95], and for windows [96–99]

It was found in Zhao et al. [91](Fig. 10(b)), that in times of strong solar radiation, the heating effect of the bifacial panels as well as the transmission of the transparent glass led to overheating of the indoor environment. However, a reflective insulation layer was installed behind the BPV modules and the level of thermal comfort indoors increased. Tina et al. [100] conducted a study evaluating the electrical and thermal performance of bifacial BIPV modules, by examining both ventilated and non-ventilated facades. Ventilated facades are able to reduce the energy consumption of a building [101], and the heat loss or gain is dependent on the properties of the ventilated cavity, such as the space between the walls [102], and the rate of airflow [103]. While monofacial PV panels used for BIPV applications are opaque, meaning that they completely shade the interior environment [100,104], BPV panels are semi-transparent making them advantageous, as they help reduce the solar gain on the façade and exploit the daylight [105,106]. Tina et al. [100] found that the operating temperature for ventilated façade integrated BIPV modules that were bifacial was lower than for the modules that were monofacial with the operating temperature 1–2 °C cooler. The power increase experienced by the BPV panels was 2.9% in comparison to the monofacial PV panels. However, when reflectors were installed, a power increase of 7.4% was experienced relative to non-ventilated monofacial panels, and a gain of 5.4% compared to ventilated monofacial panels.

Figure 11 shows the comparison in the study conducted by Tina et al. [100], which clearly indicates the advantages of using BPV for BIPV applications on

Fig. 10 Photographs of BIPV shading application and BPV applied as window shading devices.
(a) BIPV shading application (Bangalore, India) [76]; (b) photograph of BPV applied as window shading devices (Guanghan City, Deyang, China) [91].

facades due to the significantly higher energy yield, as well as the thermal fluxes showing the vast advantages of ventilated systems compared to non-ventilated systems.

Figure 12 illustrates another study [107] that investigates BPV panels in BIPV facade applications. It found an average annual bifacial gain of 22.48%. As well as the electrical production of the panels, the overall energy consumption needs of the building decreased both during the cold and warm seasons while the system was being tested. It was observed that the system permitted the management of heat transfers through the concrete wall. In the warm season, this was helped by the wall insulation, the albedo effect, and the stack effect cooling the concrete panels. In the cold season, there is a greenhouse effect in the insulated air gap.

3.3   BPV for floating PV (FPV)

FPV systems, as seen in Figs. 13 and 14, are a hot topic in solar power generation around the globe, which have emerged recently [110,111]. FPV systems hold a number of advantages, such as the fact that they do not contribute to global warming as FPV systems do not affect albedo [112], as well as reduced evaporation due to the shade provided by the system which can be between 25% and 75% depending on climatic conditions [113,114]. The effect of bifaciality can be exploited for FPV applications and may make FPV favorable for BPV modules [108]. In 2018, FPV produced 1.45 TWh of electricity and is predicted to rise up to 710 TWh per year by 2030, which is more than the current production of all PV applications [115]. This can be seen in Fig. 15.

An advantage of FPV is the decreased prevalence of the albedo effect. For land-based PV systems the ground albedo is generally lowered from 30% down to 5% due to the placement of the PV modules which can contribute to warming, the greenhouse effect, and urban heat islands. However, for FPV systems, the water surface albedo is relatively unaltered, eliminating this disadvantage [115,116]. Another advantage of FPV is its availability to be exploited at the site of hydropower sites, to utilize not only the space available but also the existing grid connections [117]. This application has already been implemented in multiple locations [118,119].

Tina et al. [108] evaluated the use of both bifacial and monofacial panels in floating applications and found that the bifacial gain was larger for locations that had a higher diffuse factor. This means that, as a rule, water surface albedo is lower at higher solar altitudes, and higher at lower solar altitudes, which means that there is a lower water surface albedo in summer months and the opposite goes for winter months [120,121]. The albedo value for many applications is taken as a specific value, which can leave errors in results of 5%–15% [121]. Hasan & Dincer [122] found in a study that when mounted in a
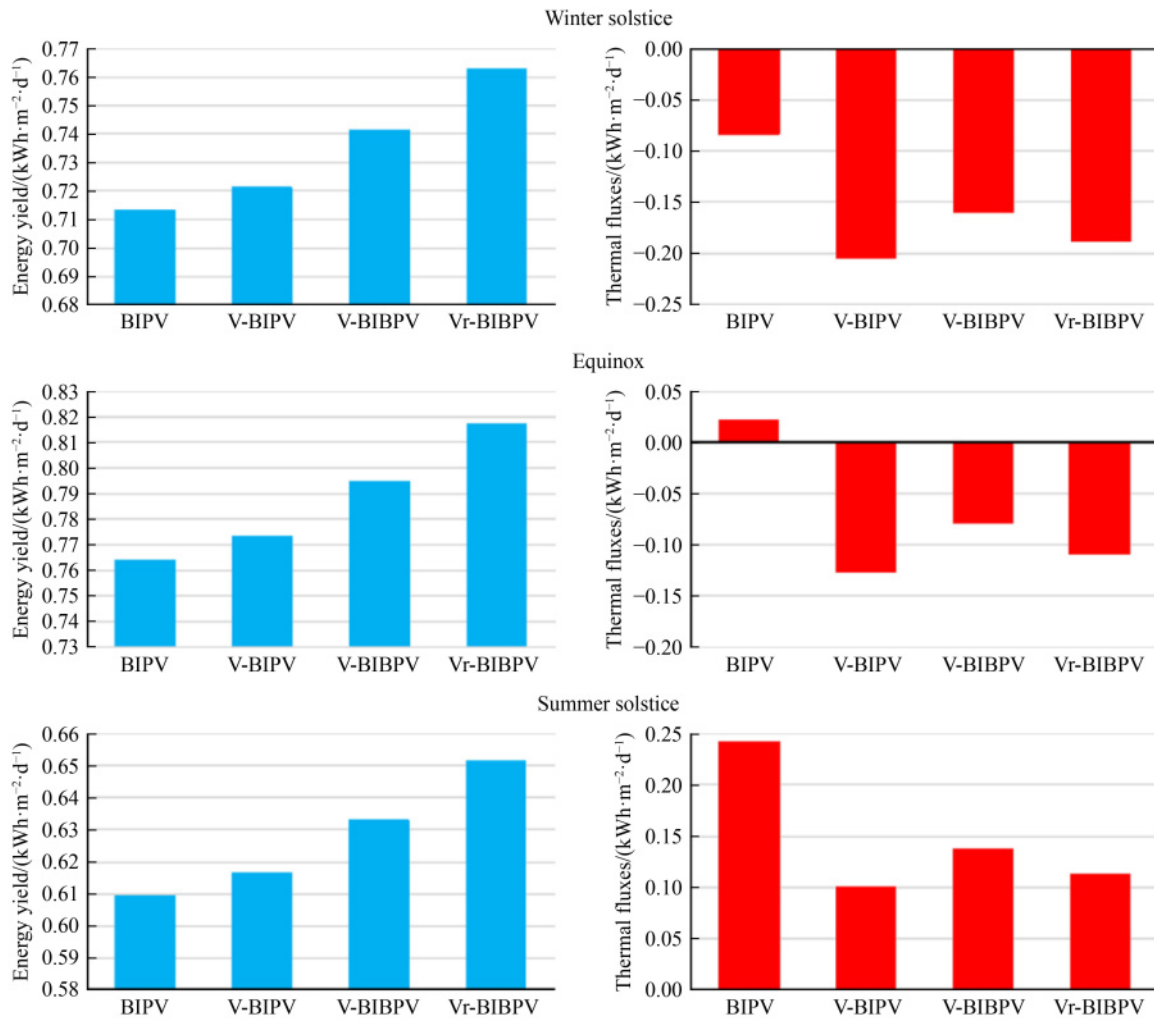
Fig. 11 Comparison of electrical energy yields and thermal fluxes for various configurations of BIPV (V-BIPV: ventilated BIPV, V-BIBPV: ventilated bifacial BIPV, Vr-BIBPV: ventilated bifacial BIPV with reflectors) (adapted with permission from Ref.[100]).
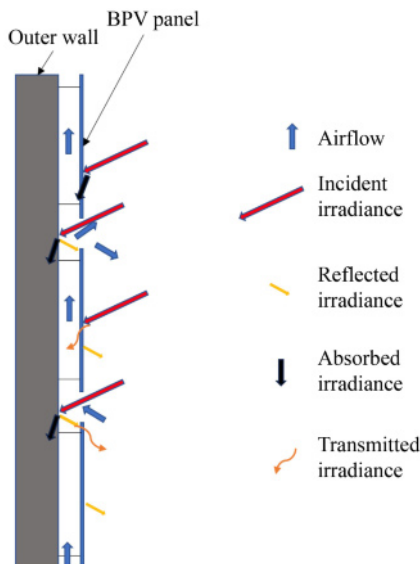

Fig. 12 Schematic example of a facade-integrated ventilated BPV system.

Fig. 13 Floating bifacial and monofacial system in Catania, Italy (adapted with permission from Ref. [108]).

north/south orientation at a tilt angle of 30°, BPV modules were able to make use of 55% more sunlight compared to their monofacial counterparts. This was reduced to 31% for an east/west orientation. A simulation simulating wavy water was also performed, reducing the values for north/south and east/west to a 49% and 33%

irradiance gain, respectively.

There is a compromise to be made with regard to FPV. While the cooling effect of the water can help lower the temperature of the PV modules and increase the electrical efficiency [109,123], the modules need to be installed at small angles of incline relative to the water surface [124]. This could nullify the benefit of the bifacial panel. Hutchins [124] also mentioned the little shelter from wind offered to a PV system on the water and the additional safety concerns that raises.

On the other hand, BPV in FPV application can face lower soiling impact which is common in most of the ground-based [125–127], and building-integrated PV [128] applications as reported elsewhere. Table 2 gives a summary of BPV applications and possible areas for improvement.

Fig. 14   448 kWp FPV at an altitude of 1800 m in Lac des Toules (adapted from Ref. [109] under the terms of CC BY license).

4   Essential equations for BPV calculations

4.1   Irradiance calculations

Calculations for BPV panels are different from those for monofacial panels. The efficiency of BPV cells is found using separate measurements for the front and rear sides, respectively [129]. Alternatively, the efficiency can be stated as an equivalent efficiency of a monofacial cell generating the same power per unit area as a BPV cell under the same test condition [31]. The bifaciality factor is commonly used, which includes the ratio of efficiencies of the front and rear side of the solar cell. The bifaciality factor is shown in Eq. (1) [31].

$$\text{Bifaciality factor } (\%) = \left(\frac{\eta_{\text{sc,front}}}{\eta_{\text{sc,rear}}}\right) \times 100. \qquad (1)$$

Efficiency can also be shown using short circuit current density (J_{sc}), which will give the separation rate (%), as shown in Eq. (2) [31,130].

$$\text{Separation rate } (\%) = \left(\frac{J_{\text{sc,front+rear}}}{J_{\text{sc,front}} + J_{\text{sc,rear}}} - 1\right) \times 100. \qquad (2)$$

The influence of the BPV panel on any parameter given as X can be given in Eq. (3) [31].

$$\Delta X = X_{\text{front+rear}} - (X_{\text{front}} + X_{\text{rear}}). \qquad (3)$$

There is no standard method for characterizing BPV cells as there is with monofacial cells [131]. The albedo, as mentioned earlier in this paper, is the key factor that affects the gain from the bifacial panel compared to a monofacial one, and can be calculated by a ratio of
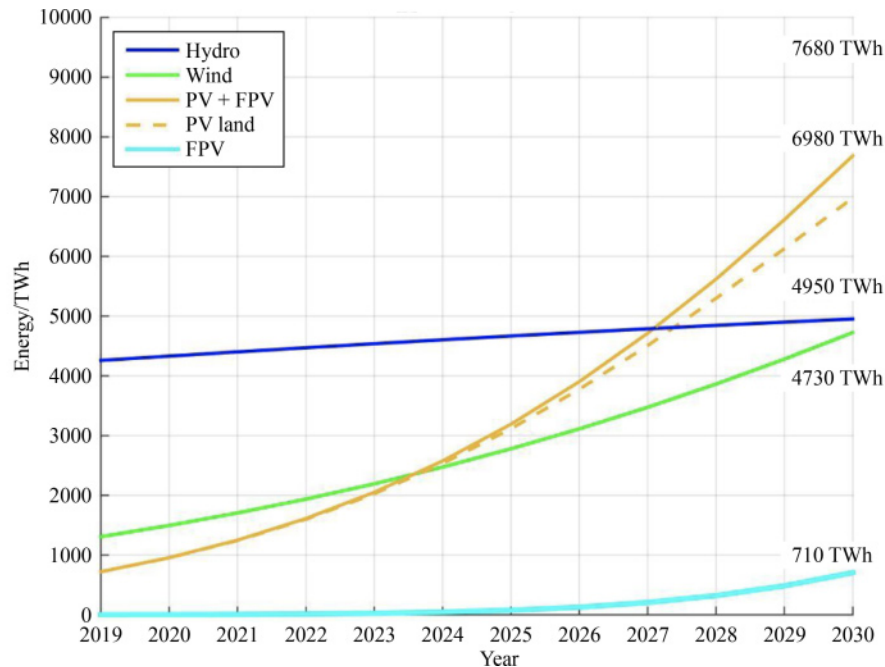

Fig. 15   Predicted growth of renewable energy systems up to 2030 (adapted with permission from Ref. [115]).

Table 2 Summary of BPV applications and possible areas for improvement

BPV application	Summary	Recommendations
Ground mounted	Most widely used type of system for commercial PV systems. Can produce unique energy generation profile depending on how the panels are mounted. Panel-to-panel shading must be eradicated to maximize the bifacial gain. When the angle of the panel to the ground is 20°, incident irradiation on the rear side of the panel is negligible. Ground sculpting can produce a significant bifacial gain	Standardized irradiance model would be useful for the industry
BAPV	Good for use of green roofs when mounted vertically, as they can support both PV generation and vegetation simultaneously. Not useful for conventional roof mounted panels on slanted roofs with panels mounted parallel to the roof as rear side irradiance will be negligible	Roofs should be made with reflective materials to increase the albedo value and to decrease the cooling load of the building
BIPV	Semi-transparent BPV panels can help reduce solar gain, and exploit daylight unlike opaque monofacial panels. Power gain can also be experienced when swapping monofacial for BPV ventilated facade integrated BIPV modules	Work into making BIPV more aesthetically pleasing or less visually prominent should be done
APV	APV can help increase crop yield for certain crops and decrease soil evaporation. Vertically mounted BPV panels can boost both energy production and crop yield	Work on what crops are ideal for BPV based APV should be done
FPV	The use of BPV is more advantageous in locations with a higher diffuse factor, meaning a higher water surface albedo at lower solar altitudes. A sweet spot must be found between maximizing the use of the rear side irradiance and making the most of the cooling effect of the water	Increasing the tilt of the panel to increasing the waters cooling effect can nullify the benefit of the bifacial panel. Possible ways to avoid this could be looked into

horizontal reflected irradiance (HRI), and global horizontal irradiance (GHI) [132,133], as given in Eq. (4) [132,133].

$$\text{Albedo} = \frac{\text{HRI}}{\text{GHI}}. \tag{4}$$

The light incident on a panel comes from both direct and diffuse radiation. The level of front and rear irradiance can be calculated in W/m². Front irradiance can be defined in Eq. (5) [134].

$$I_{\text{f}} = I_{\text{dir,f}} + I_{\text{gnd,f}} + I_{\text{diff,f}}, \tag{5}$$

where $I_{\text{dir,f}}$ is the direct irradiance, $I_{\text{gnd,f}}$ is the ground reflected irradiance, and $I_{\text{diff,f}}$ is diffuse irradiance.

Figure 16 helps demonstrate the following equations to help visualize the factors affecting the levels of irradiance incident on the front or rear side of a panel. In Fig. 16, A_{m} represents the module azimuth, θ_{m} represents the module tilt angle, A_{s} is the sun azimuth, and z is the zenith angle. The components of the equation for front side irradiance can be defined in Eq. (6) [134].

$$I_{\text{dir,f}} = \text{DNI} \times \cos \text{AOI}_{\text{f}} \times rl_{\text{dir,f}}, \tag{6}$$

where AOI_{f} (°) represents the angle of incidence between direct normal irradiation (DNI) radiation and the normal to the front surface of the module, which can be seen in Eq. (7) [134].

$$\cos \text{AOI}_{\text{f}} = (\cos z \times \cos \theta_{\text{m}} + \sin z \times \sin \theta_{\text{m}} \times \cos (A_{\text{s}} - A_{\text{m}})), \tag{7}$$

where $rl_{\text{dir,f}}$ is the reflection losses of light reaching the front face of the PV module for $I_{\text{dir,f}}$ irradiance. It is quantified by Eq. (8) in Ref. [135].

$$rl_{\text{dir,f}} = \frac{1 - \exp\left(-\cos\left(\dfrac{\text{AOI}_{\text{f}}}{a_{\text{r}}}\right)\right)}{1 - \exp\left(\dfrac{-1}{a_{\text{r}}}\right)}, \tag{8}$$

where a_{r} is the angular loss coefficient, which is an empirical dimensionless parameter and is generally
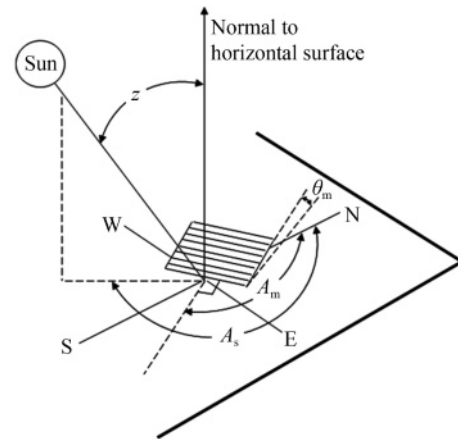

Fig. 16 Solar panel module and sun angles of interest (adapted with permission from Ref. [134]).

0.16–0.17 for commercial clean a-Si modules, or 0.20 if the modules surface has a moderate quantity of dust [136]. $I_{\text{gnd,f}}$ can be calculated by Eq. (9) in Ref. [134].

$$I_{\text{gnd,f}} = \text{GHI} \times \rho \times gvf \times rl_{\text{gnd,f}}, \tag{9}$$

where ρ is the ground albedo, and gvf is the ground view factor, which can be calculated by Eq. (10) in Ref. [137].

$$gvf = \frac{1 - \cos \theta_{\text{m}}}{2}, \tag{10}$$

and $rl_{\text{gnd,f}}$ represents the reflection losses of the light reaching the front surface of the module for $I_{\text{gnd,f}}$, whose value depends on the module tilt angle. The relation between $rl_{\text{gnd,f}}$ and module tilt angle can be seen in Fig. 17.

For the final component of the equation for irradiance on the front side of the panel, $I_{\text{diff,f}}$ can be defined by Eq. (11) in Ref. [134].

$$I_{\text{diff,f}} = \text{DHI} \times svf, \tag{11}$$

where DHI is the diffuse horizontal irradiance, svf is the sky view factor [138] which presents the Perez model as
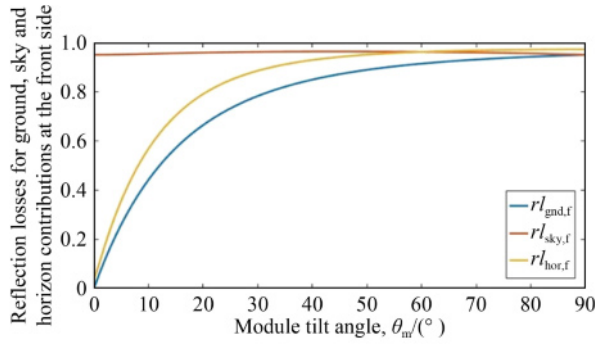
Fig. 17 Effect of module tilt angles and reflection losses (adapted with permission from Ref. [134]).

a good way to calculate the sky view factor. Given Eq. (12) in Ref. [134].

$$svf = (1 - F_1) \times \frac{1 + \cos\theta_m}{2} \times rl_{sky,f} + F_1 \times \frac{a'}{c'} \times rl_{cir,f} + |F_2 \times \sin\theta_m \times rl_{hor,f}|, \quad (12)$$

where $rl_{sky,f}$ is front side reflection loss for sky contribution, $rl_{cir,f}$ is front side reflection loss for circumsolar component, $rl_{hor,f}$ is front side reflection loss for horizontal contribution, F_1, F_2, a', and c' are coefficients expressing both the degree of circumsolar and horizon anisotropy, and sky geometry parameters, defined by Eqs. (13)–(18) in Ref. [138].

$$F_1 = F_{11}(\varepsilon') + \Delta F_{12}(\varepsilon') + zF_{13}(\varepsilon'), \quad (13)$$

$$F_2 = F_{21}(\varepsilon') + \Delta F_{22}(\varepsilon') + zF_{23}(\varepsilon'), \quad (14)$$

$$\varepsilon' = \frac{DHI + DNI}{DHI}, \quad (15)$$

$$\Delta = \frac{DHI}{E_0 \cos z}, \quad (16)$$

$$a' = 2(1 - \cos\alpha)\chi_c, \quad (17)$$

$$c' = 2(1 - \cos\alpha)\chi_h. \quad (18)$$

These equations are derived from the Perez models [139–142]. For Eqs. (13)–(18), ε' is the clearness of the sky as in Perez's study [140], Δ is the brightness of the sky, D_h is DHI, E_0 is extra-terrestrial normal irradiance, and χ_c and χ_h can be defined by Eqs. (20)–(23) in Ref. [138].

$$\chi_c = \begin{cases} \psi_h \cos\theta, & \text{if } \theta < \frac{\pi}{2} - \alpha, \\ \psi_h \psi_c \sin(\psi_c \alpha), & \text{if } \theta \in [\pi \pm \alpha] \\ 0, & \text{otherwise,} \end{cases} \quad (20)$$

$$\chi_h = \begin{cases} \cos z, & \text{if } z < \frac{\pi}{2} - \alpha, \\ \psi_h \sin(\psi_h \alpha), & \text{otherwise,} \end{cases} \quad (21)$$

$$\psi_c = \frac{\frac{\pi}{2} - \theta + \alpha}{2\alpha}, \quad (22)$$

$$\psi_h = \begin{cases} \frac{\frac{\pi}{2} - z + \alpha}{2\alpha}, & \text{if } z < \frac{\pi}{2} - \alpha, \\ 1, & \text{otherwise,} \end{cases} \quad (23)$$

where θ is the incidence angle (rad). For the coefficients of F in Eqs. 13 and 14 [138], Table 3 provides values for varying levels of ε'. It should be noted that the circumsolar angle is taken to be 25° for these calculations [140], as listed in Table 3.

For estimated reflection losses of $rl_{hor,f}$ and $rl_{cir,f}$, Ref. [143] can be applied, using Fig. 17 to estimate the losses based on the module tilt angle.

For rear side irradiance, a similar equation can be used for front side irradiance, as expressed by Eq. (24) in Ref. [134].

$$I_r = I_{dir,r} + I_{gnd,r} + I_{diff,r}. \quad (24)$$

Direct and diffuse radiation ($I_{dir,r}$ and $I_{diff,r}$) can be calculated by the same approach used for front side irradiance [134,144–146]. One change needed, however, is that θ_m should be changed to be $\theta_m + 180°$. The value for $I_{gnd,r}$ becomes more complex due to the additional factors affecting rear ground reflected irradiance, such as the shadow cast on the ground by the panel itself. The following method is derived from the assumption that PV rows consist of at least 12 solar modules [134]. $I_{gnd,r}$ can be calculated by Eq. (25) in Ref. [134].

$$I_{gnd,r} = \sum_{i=1°}^{180° - \theta_m} \rho \times GRI^i \times CF^i \times rl_{gnd,r}^{(i)}, \quad (25)$$

where

$$GRI^i =$$

$$\begin{cases} \text{If ground is shaded} : DNI \times F_1 \times \frac{a'}{c'} + CF_{sky} \times DHI \times (1 - F_1), \\ \text{If ground is unshaded} : CF_{sky} \times DHI \times (1 - F_1), \end{cases} \quad (26)$$

$$CF_{sky} = \frac{1}{2} \times (1 - \cos\sigma), \quad (27)$$

$$\sigma = \begin{cases} \Phi, & \Phi > 0, \\ \Phi + 180°, & \text{otherwise,} \end{cases} \quad (28)$$

$$\Phi = \tan^{-1}\left(\frac{h_{mg} + l_m \sin\theta_m}{\left(\frac{h_{mg}}{\sin\theta_m} + l_m\right) \times \cos\theta_m - x^{(i)}}\right), \quad (29)$$

$$x^{(i)} = \frac{\sin i \times \left(\frac{h_{mg}}{\sin\theta_m} + \frac{l_m}{2}\right)}{\sin(180° - i - \theta_m)}, \quad (30)$$

where l_m is the module length in meters, and h_{mg} is the module height in meters between the lowest edge of the module and the ground, and CF^i is the configuration factor for the ith in Eq. (31) [134].

$$CF^i = \frac{1}{2} \times (\cos(i-1) - \cos i). \tag{31}$$

It should be noted that BPV systems are much newer than their monofacial counterparts, and as such there are still new methods being developed in order to calculate the irradiance incident on the rear side of the panel [147,148]. While most methods differ slightly, they will all operate under the same principles, taking into account direct, diffuse, and ground reflected irradiance. To calculate the ground reflected irradiance, it is essential to know the albedo which can be calculated at a desired site as in Ref. [149]. However, it is helpful to have a list of general albedo values for rough irradiance estimations, as given in Table 4.

4.2 Electrical performance analysis

The electrical performance of a panel is important to understand. For assessing the performance of a panel, but also in order to be able to compare a bifacial panel to a conventional monofacial panel, a diode equivalent circuit is a useful way to analyze the electrical performance of a solar cell. Reducing the number of calculations and components needed to analyze. Figures 18 and 19 demonstrate diode equivalent circuits for both conventional monofacial panels, and bifacial panels, respectively. Noticing that the bifacial diagram essentially has two of the monofacial circuits for both the front and rear faces of the panel.

For Fig. 19, it should be noted that the bifacial module can also be modeled by a 2-diode model, consisting of a second diode in parallel with the current source [155]. The $I-V$ relationship for the circuit is given by Eq. (32) in Ref. [155], and an example of the $I-V$ curves for a BPV module can be seen in Fig. 20.
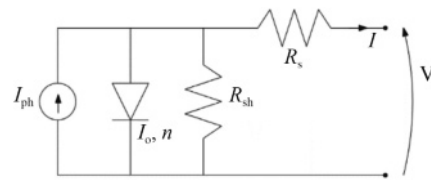
Table 3 Coefficients needed for irradiance calculations [140]

ε'	F_{11}	F_{12}	F_{13}	F_{21}	F_{22}	F_{23}
1–1.056	−0.011	0.748	−0.080	−0.048	0.073	−0.024
1.056–1.253	−0.038	1.115	−0.109	−0.023	0.106	−0.037
1.253–1.586	0.166	0.909	−0.179	0.062	−0.021	−0.050
1.586–2.134	0.419	0.646	−0.262	0.140	−0.167	−0.042
2.134–3.23	0.710	0.025	−0.290	0.243	−0.511	−0.004
3.23–5.98	0.857	−0.370	−0.279	0.267	−0.792	0.076
5.98–10.08	0.743	−0.073	−0.228	0.231	−1.180	0.199
10.08–∞	0.421	−0.661	0.097	0.119	−2.125	0.446

Table 4 Albedo values of common surfaces

Surface material	Albedo value	Source
Sand (wet)	0.09	Bradley et al. [150]
Slate	0.1	Taha et al. [151]
Gravel	0.12	Du et al. [121]
Asphalt	0.125	Taha et al. [151]
Corrugated iron	0.13	Taha et al. [151]
Water	0.14	Rosenberg et al. [152]
Wood	0.15	Taha et al. [151]
Sand (dry)	0.18	Bradley et al. [150]
Grass	0.205	Taha et al. [151]
Concrete	0.225	Taha et al. [151]
Field (bare)	0.12–0.25	Bradley et al. [150]
Stone	0.275	Taha et al. [151]
Brick	0.3	Taha et al. [151]
Soil (dry sandy)	0.25–0.45	Radionov et al. [153]
Gravel (white)	0.65	Du et al. [121]
Snow (2–5 d old)	0.75–0.8	Laudani et al. [154]
Snow (fresh)	0.8–0.88	Laudani et al. [154]

Fig. 18 Diode equivalent circuit for a conventional monofacial solar cell (adapted with permission from Ref. [154]).
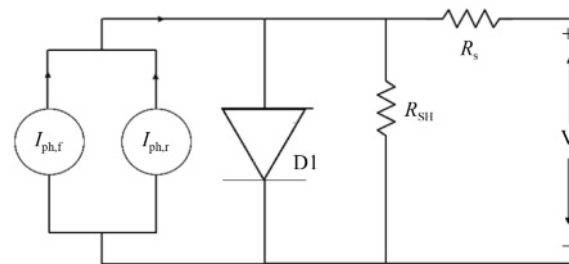

Fig. 19 1-diode equivalent circuit for a bifacial solar cell (adapted with permission from Ref. [40]).
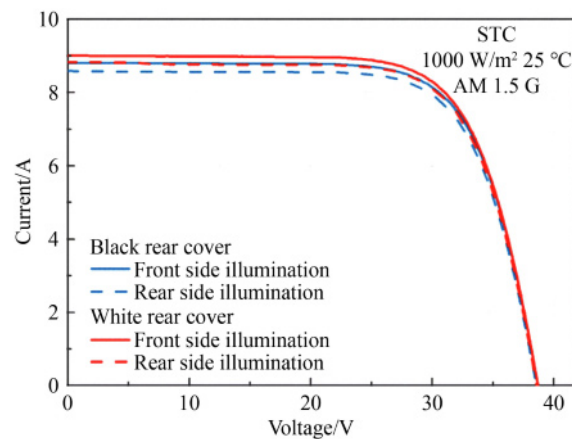

Fig. 20 Example of the current voltage relationship (adapted from Ref. [156] under the terms of CC BY license).

$$I = I_{ph(F+R)} - I_0 \left(\exp\left(\frac{V + IR_s}{N_s n V_t} \right) - 1 \right) - \frac{V + IR_s}{R_{SH}}, \quad (32)$$

where R_s is the series resistance, R_{SH} is the shunt resistance, N_s is the number of cells, n is the diode ideality factor, V_t is the thermal voltage, and I_0 is the reverse saturation current.

Energy production from a bifacial PV panel can be calculated by Eq. (33) in Ref. [157].

$$P_{PV} = \frac{P_{STC,f} \times (I_f + I_r \times b) \times f_1}{1000} \times (1 + \gamma \times (T_c - 25))$$
$$\times \eta_{inv} \times (1 - \beta_0 - y \times \beta_1) \times (1 - l), \quad (33)$$

where $P_{STC,f}$ is the power production of the panels with light reaching their front side only, under standard test conditions, b is the bifaciality factor, f_1 is the spectral irradiance contribution, γ is the power temperature coefficient, and T_c is the cell temperature. For consideration of the cell degradation, β_0 is the initial cell degradation, and β_1 is the yearly degradation rate of the panel, with y being the age of the panel in years at the time of analysis. The parameter l combines other losses such as shading and ohmic losses. Solar spectral irradiance (f_1) changes throughout the day, which influences the modules performance [134], particularly high band gap semiconductor materials [158,159]. It can be represented empirically by Eq. (34) in Refs. [158,159].

$$f_1 = a_0 \times a_1 \times AM_a + a_2 \times (AM_a)^2 + a_3 \times (AM_a)^3 + a_4 \times (AM_a)^4. \quad (34)$$

AM_a corresponds to the absolute air mass, which can be approximated using Eq. (35) in Ref. [160].

$$AM_a \approx e^{(-0.0001184 \times El)} \times AM, \quad (35)$$

where AM is the air mass based on Kasten's study [161] from which accurate results can be obtained for zenith angles up to 90° by Eq. (36) in Ref. [134].

$$AM = \frac{1}{\cos z + 0.50572 \times (96.07995° - z)^{-1.6364}}. \quad (36)$$

T_c is based on Eq. (37) in Ref. [157].

$$T_c = T_a + \frac{I_f + I_r}{800} \times (T_{INOCT} - 20), \quad (37)$$

where T_a is the ambient temperature, and T_{INOCT} is the panels installed normal operating temperature, which depends on the mounting structure, as this will affect the heat dissipation of the solar cell [162], and I_f and I_r are the front and rear irradiances on the panel faces respectively.

$$T_{INOCT} = T_{NOCT} + x_{mount}, \quad (38)$$

where T_{NOCT} is the normal operating temperature of the cell, and x_{mount} is a coefficient whose value is based on the selected mounting structure [134].

Over the course of time, PV systems will degrade, and their electrical power output will decrease. PV manufacturers will guarantee a degradation trend that is generally linear, and will be expressed in %/a. This will be required for the system to fall within its warranty, which should not exceed 0.8% per year [163]. However, Ref. [164] reported cases where PV plants degradation rate exceeded 0.8% per year after 10 years due to environmental factors such as high humidity and ambient temperatures. Likewise, Theristis et al. [165] reported the degradation of recent PV technologies. Notably, 6 out of 23 systems will fail to meet the terms set in the warranty. According to da Silva et al. [166], BPV modules are less susceptible to light and elevated temperature induced degradation. While monofacial and BPV modules are more susceptible to different types of degradation [166]. da Silva et al. [166] identified that microcracking, and soiling were both the top two most significant contributors for both types of the technology. In order to avoid instances of micro cracking and soiling, work is being done on technologies such as pre stressing, dust shielding, and hydrophobic coatings [167–169].

5 Cost considerations

Rodríguez-Gallegos et al. [170] conducted a worldwide study and found that BPV systems with single axis trackers produced the lowest LCOE in the vast majority of locations. LCOE is defined as the price that electricity should be sold in order for a system to break even at the end of its lifetime [171]. Dual axis trackers produced a higher energy yield. However, the initial investment was higher. This can be seen in Fig. 21, as the cost for a dual axis tracker is significantly more than for both fixed tilt and single axis per W_p.

Table 5 gives an example of the LOCE of different PV systems at different locations around the world in USD cents/kWh [170], which clearly shows places where it is cheaper to operate a PV system, and that a bifacial
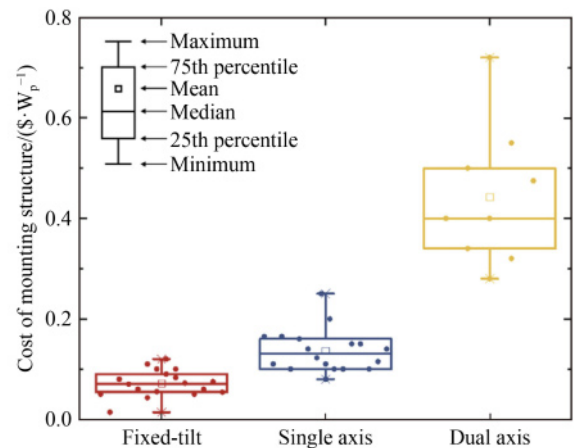

Fig. 21 Cost of different PV mounting structures (adapted with permission from Ref. [170]).

Table 5 LCOE for various PV applications in different locations [170]

	Monofacial-fixed	Bifacial-fixed	Monofacial-1 axis	Bifacial-1 axis	Monofacial-2 axis	Bifacial-2 axis
China (Zhongba)	2.9 ± 0.5	2.8 ± 0.4	2.4 ± 0.4	2.4 ± 0.4	3.1 ± 0.7	3.1 ± 0.6
USA (Yuma)	4.8 ± 0.7	4.5 ± 0.6	4.0 ± 0.6	3.9 ± 0.5	4.8 ± 0.9	4.6 ± 0.8
Japan (Mine)	5.0 ± 0.7	4.7 ± 0.6	4.6 ± 0.7	4.3 ± 0.6	5.5 ± 1.0	5.1 ± 0.8
Germany (Dornstetten)	6.9 ± 1.0	6.2 ± 0.8	6.0 ± 0.9	5.6 ± 0.7	7.0 ± 1.3	6.5 ± 1.0
India (Kavalanahalli)	4.8 ± 0.9	4.7 ± 0.8	4.3 ± 0.8	4.1 ± 0.7	5.6 ± 1.3	5.4 ± 1.1
Italy (St. Biagio Platani)	5.2 ± 0.8	4.8 ± 0.7	4.5 ± 0.7	4.2 ± 0.6	5.5 ± 1.1	5.2 ± 0.9
UK (Liskeard)	8.4 ± 1.2	7.6 ± 0.9	7.3 ± 1.1	6.8 ± 0.8	8.5 ± 1.5	7.9 ± 1.2
Australia (St. George Ranges)	6.2 ± 0.9	5.9 ± 0.7	5.2 ± 0.8	5.0 ± 0.6	5.8 ± 1.0	5.6 ± 0.8
France (Meyreuil)	5.8 ± 0.9	5.4 ± 0.6	4.9 ± 0.8	4.7 ± 0.6	5.6 ± 1.0	5.4 ± 0.8
Republic of Korea (Uiseong County)	5.7 ± 0.9	5.3 ± 0.7	5.1 ± 0.8	4.8 ± 0.6	6.1 ± 1.2	5.7 ± 1.0

system with a single axis tracker will deliver the lowest LCOE.

A detailed cost estimation method is explained in Rodríguez-Gallegos et al. [134], as demonstrated below, where the initial investment cost can be defined by Eq. (40).

$$C_{ini,inv} = P_{stc,f} \times \left(c_{sp} + c_{ins} + c_{ivt}^{(0)} \right), \quad (40)$$

in which c_{sp} ($/Wp) is equal to the cost of the solar panels, c_{ins} ($/Wp) is the installation cost, $c_{ivt}^{(0)}$ ($/Wp) is equal to the cost of the inverter, and c_{ins} can be divided into two groups of material costs ($c_{ins,mat}$) and labor costs ($c_{ins,lab}$), which is given in Eq. (41).

$$c_{ins} = c_{ins,mat} + c_{ins,lab}. \quad (41)$$

Warranty extension costs c_{war} ($) can also be considered with respect to the PV inverter [172,173]. For an inverter warranty w_{inv} at its ith warranty extension, a percentage of the cost of the inverter must be covered $\pi_{ivt}^{(i \times w^{PV})}$ (%). This can be shown by Eq. (42).

$$C_{war} = \sum_{i=1}^{\lfloor l_S / w_{ivt} \rfloor} P_{STC,f} \times c_{ivt}^{i \times w_{ivt}} \times \pi_{ivt}^{i \times w_{ivt}} \times \frac{(1+IR)^{i \times w_{ivt}}}{(1+DR)^{i \times w_{ivt}}}, \quad (42)$$

where $c_{ivt}^{i \times w_{ivt}}$ ($/Wp) is equal to the cost of the inverter at the year $i \times w_{ivt}$, l_S / w_{ivt} is equal to the number of times that the warranty needs to be extended over a lifetime of l_S years, and IR (%) and DR (%) are inflation rates and discount rates respectively. The total cost of a PV system throughout its lifetime can be calculated by Eq. (43).

$$C_{PV} = C_{Bank,int} + C_{Bank,amor} + C_{own} + C_{war} + C_{insu} + C_{OM}, \quad (43)$$

where $C_{Bank,int}$ is the interest paid on loans taken, $C_{Bank,amor}$ is the amortization of the given loans, C_{own} is the portion of the initial investment required to be paid that is not covered by the loans given, C_{war} is given in Eq. (42), C_{insu} is the cost to insure the system, and C_{OM} is the operation and maintenance costs of the system. These variables are explained in more detail in Rodríguez-Gallegos et al. [134].

6 Discussion

6.1 Future of BPV in the industry

As demonstrated earlier in Figs. 4 and 5, the influence of BPV in the photovoltaic market is growing significantly, and although it still holds a minority stake in the industry, it is expected to dominate the photovoltaic market in the future. Figure 4 shows that by 2030, BPV should occupy approximately 70% of the market.

6.2 Future needs for BPV policy

The policy for supporting PV projects is generally not specific to BPV projects, instead, the policy for supporting projects encompasses all solar PV technologies such as bifacial and monofacial alike, and does not differentiate between the two. Appropriate policy is necessary for the advancement and innovation of the PV industry [174–176]. Up to this point, governments have supported PV innovation through feed in tariffs, renewable portfolio standards, and tax incentives [177]. Existing policies drive innovation through lowering the cost of use and increasing the demand for PV power [168]. These policies have been shown to be effective [178–181]. Policies specific to BPV systems could boost the advancement and adoption of the technology, as previously done with monofacial panels. In order for BPV to be at the forefront of the industry, there needs to be specific support in place at the scale of government, and industry leaders. This will help lead the way for standardization in the technology at a scale seen currently for monofacial PV from the likes of the IEC. Future applications for PV systems should look to be supported such as electric vehicle charging stations as the transport industry is a significant contributor to GHG and global warming. In order for the EV industry to be truly green, however, it must be powered by renewable electricity [182–184], such as BPV EV charging stations [185].

6.3 BPV application summary and future needs

While BPV is proven as a genuinely viable solution to the need for the rapid expansion of renewable energy sources, there is still work that needs to be done.

6.3.1 Ground mounted

Ground mounted systems are the most widely used worldwide. Because of this, ground mounted BPV has benefited from the most amount of research to date whether it be modeling or experimental research for optimization. BPV systems are generally able to add 25%–30% additional power output compared to conventional monofacial panel when the configuration is optimized and is shown earlier that single axis tracked BPV systems deliver the lowest LCOE. The BPV modules must generally be mounted higher than monofacial modules due to the need for rear irradiance contribution. BPV mounting configurations can vary more then monofacial systems, with vertically mounted systems proven to be useful for BPV systems by producing a generation profile more similar to that of the demand profile seen throughout the day. In all regions of the world, vertical BPV modules are able to outperform monofacial panels.

Despite the advantages mentioned above, there is still work to be done in improving the technologies of ground-mounted applications. Due to the novelty of the technology, there are many types of modeling methods available from both open-source and commercial backgrounds, all using either view factor or ray tracing methods. The industry would benefit from a standardized method for calculating BPV irradiance.

6.3.2 BAPV

Monofacial BAPV is already widely rolled out on domestic and commercial rooftops. Green roofs look most promising for bifacial BAPV applications, specifically vertically mounted BPV. Vertically mounted BPV-BAPV systems are able to give specific energy yields comparable to standard flat roof systems. However, a low ground coverage ratio is required to avoid panel-to-panel shading. To maximize green roofs, vertical BPV panels should be used. However, for a normal flat roof, conventional tilted mounting should be used. For angled roofs, there is no evidence of BPV being used to date. Many examples of BPV applications for BAPV are for vertical systems of green roofs, future work focusing on conventional flat roofs, with various reflectance coatings that would be valuable in order to determine commercial viability and benefit compared to monofacial systems.

6.3.3 BIPV

Very novel application and much work needs to be done in order to validate the technology for commercially viable applications. Ventilated BPV facades operate at lower temperatures than ventilated monofacial BIPV facades, leading to a further increased bifacial gain. Bifacial BIPV can yield an annual bifacial gain of 22.48% and can help decrease the energy consumption of building through albedo, greenhouse, and stack effect throughout different seasons. Work on making BPV for BIPV applications less visually prominent would make the product more commercially viable.

6.3.4 Agrivoltaics

PV panels mounted over vegetation even at heights of 4 m can have significantly lowered cell temperature than panels mounted over normal ground. Rear side irradiance homogeneity is increased due to the larger ground clearance in agri-PV. Different crops have specific albedo values. This means that some crops are more suitable to bifacial agrivoltaics than others. Vertically mounted BPV modules can increase both energy and crop yield. As of yet, there is no work on crop optimization for bifacial agrivoltaics. This would be useful to determine what crops produce the greatest yield increase when used with BPV, and what crops increase the energy production of BPV systems most for tilted and vertical systems.

6.3.5 FPV

FPV is a more novel application of photovoltaics than some others. Bifacial gain is higher in locations with a higher diffuse factor. Water surface evaporation can be reduced by 25%–75%, and the relatively unchanged albedo effect can lead to lesser effects on global warming. BPV modules for FPV can make use of up to 55% more sunlight than monofacial counterparts. However, there is a lack of opportunity for sheltering FPV systems from wind, which becomes more prominent with BPV modules having to be mounted higher on the surface to maximize rear side irradiance. Mounting the panels close to water in order to maximize cooling can help with this. However, may nullify the benefits of bifaciality. For future research, dedicated modeling software for floating BPV would be useful, as well as the need for long-term assessment of BPV use in floating applications.

7 Conclusions

This review has analyzed research and review papers

examining the performance of many different BPV set ups of different applications in different areas of the world. It outlines the findings from studies conducted, such as the optimal configuration and level of equipment for various applications. For example, for ground mounted BPV, single axis tracked systems are able to deliver the lowest LCOE in all sampled regions of the world. This review also suggests areas of the industry in which development and research is most needed, providing the scope and suggestions to look further into the technology. Overall, BPV can provide advantages compared to monofacial systems all round the world, in all major applications. Though the advantages are not only limited to increased electricity production, there are secondary benefits to the technology, ranging from enhanced crop growth and reduced water evaporation when applied for APV, reduced reservoir water evaporation when used for FPV systems, as well as the option for alternative energy generation profiles for vertical BPV systems. These advantages, as well as the others mentioned in this paper show great versatility and future potential for the BPV technology. However, what has been demonstrated thus far is just the start. Work must start in the industry to begin the standardization of the technology. Industry leaders must do what has already been done for the monofacial technology in order to make it both more reputable and commercially attractive.

Competing interests The authors declare they have no competing interests.

Notations

a'	Sky geometry factor according to Perez model
a_r	Angular loss coefficient
AM	Air mass
AM_a	Absolute air mass
A_m	Module azimuth angle/(°)
A_s	Sun azimuth angle/(°)
AOI_f	Front side angle of incidence/(°)
b	Bifaciality factor
c'	Sky geometry factor according to Perez model
$C_{ini,inv}$	Cost of initial investment/\$
c_{ins}	Installation cost/\$
$c_{ins,lab}$	Labor costs/\$
$c_{ins,mat}$	Material costs/\$
$c_{ivt}^{(0)}$	Inverter cost/\$
c_{sp}	Cost of solar panels/\$
C_{war}	Warranty extension cost/\$
CF^i	Configuration factor for ith segment
CF_{sky}	Sky configuration factor
DNI	Direct normal irradiance/(W·m^{-2})
DR	Discount rate/%
E_0	Extra-terrestrial normal irradiance/(W·m^{-2})
f_1	Spectral irradiance contribution
F_1	Coefficient expressing degree of circumsolar and horizon anisotropy
F_2	Coefficient expressing degree of circumsolar and horizon anistropy
GHI	Global horizontal irradiance/(W·m^{-2})
GRI^i	Ground reflected irradiance for ith segment
gvf	Ground view factor
h_{mg}	Module height/m
HRI	Horizontal reflected irradiance/(W·m^{-2})
I	Current generated/A
I_0	Reverse saturation current/A
$I_{diff,f}$	Front side diffuse irradiance/(W·m^{-2})
$I_{diff,r}$	Rear side diffuse irradiance/(W·m^{-2})
$I_{dir,f}$	Front side direct irradiance/(W·m^{-2})
$I_{dir,r}$	Rear side direct irradiance/(W·m^{-2})
I_f	Front side irradiance/(W·m^{-2})
$I_{gnd,f}$	Front side ground reflected irradiance/(W·m^{-2})
$I_{gnd,r}$	Rear side ground reflected irradiance/(W·m^{-2})
$I_{ph(F+R)}$	Front + rear photogenerated current/A
I_r	Rear side irradiance/(W·m^{-2})
IR	Inflation rate/%
$J_{sc,front}$	Short circuit current density of front side/(mA·cm^{-2})
$J_{sc,rear}$	Short circuit current density of rear side/(mA·cm^{-2})
l_m	Module length/m
l_S	System lifetime/year
l_S/w_{ivt}	Number of warranty extensions over lifetime
n	Diode ideality factor
N_s	Number of cells
P_{PV}	PV power production/W
$P_{STC,f}$	Front side power production at STC/W
R_s	Series resistance/Ω
P_{SH}	Shunt resistance/Ω
$rl_{cir,f}$	Front side reflection loss for circumsolar component

$rl_{\text{dir,f}}$	Reflection loss for direct front side irradiance
$rl_{\text{hor,f}}$	Front side reflection loss for horizontal contribution
$rl_{\text{sky,f}}$	Front side reflection loss for sky contribution
svf	Sky view factor
T_a	Ambient air temperature/°C
T_c	Cell temperature/°C
T_{INOCT}	PV panel installed normal operating temperature/°C
V	Voltage/V
V_t	Thermal voltage/V
x_{mount}	Coefficient based on selected mounting structure
y	Age of panel/year
z	Sun zenith angle/(°)
a	Circumsolar half angle/rad
β_0	Initial cell degradation/%
β_1	Yearly degradation rate/$(\% \cdot \text{year}^{-1})$
γ	Power temperature coefficient/$(\% \cdot {}^{\circ}\text{C}^{-1})$
$\eta_{\text{sc,front}}$	Front side efficiency/%
$\eta_{\text{sc,rear}}$	Rear side efficiency/%
θ_m	Module tilt angle/(°)
ρ	Ground albedo
ε'	Sky clearness
Δ	Sky brightness
$\chi_c, \chi_h, \psi_h, \psi_c$	Intermediate parameters in Perez model

References

1. Kuşkaya S, Bilgili F, Muğaloğlu E, et al. The role of solar energy usage in environmental sustainability: Fresh evidence through time−frequency analyses. Renewable Energy, 2023, 206: 858–871

2. Chandio A A, Shah M I, Sethi N, et al. Assessing the effect of climate change and financial development on agricultural production in asean-4: The role of renewable energy, institutional quality, and human capital as moderators. Environmental Science and Pollution Research International, 2022, 29(9): 13211–13225

3. Assi A F, Zhakanova Isiksal A, Tursoy T. Renewable energy consumption, financial development, environmental pollution, and innovations in the ASEAN + 3 group: Evidence from (P-ARDL) model. Renewable Energy, 2021, 165: 689–700

4. Karaaslan A, Çamkaya S. The relationship between CO_2 emissions, economic growth, health expenditure, and renewable and non-renewable energy consumption: Empirical evidence from turkey. Renewable Energy, 2022, 190: 457–466

5. Liu H, Khan I, Zakari A, et al. Roles of trilemma in the world energy sector and transition towards sustainable energy: A study of economic growth and the environment. Energy Policy, 2022, 170: 113238

6. IEA. Global energy review 2021. 2023–9–28, available at the website of IEA

7. IEA. Global energy review 2022. 2023–9–28, available at the website of IEA

8. Liu W, Shen, Y, Razzaq A. How renewable energy investment, environmental regulations, and financial development derive renewable energy transition: Evidence from G7 countries. Renewable Energy, 2023, 206: 1188–1197

9. Taghizadeh-Hesary F, Yoshino N. The way to induce private participation in green finance and investment. Finance Research Letters, 2019, 31: 98–103

10. Wu H. Evaluating the role of renewable energy investment resources and green finance on the economic performance: evidence from OECD economies. Resources Policy, 2023, 80: 103149

11. IPCC. Climate Change 2022—Mitigation of Climate Change: Working Group III Contribution to the Sixth Assessment Report of the Intergovernmental Panel on Climate Change. Cambridge: Cambridge University Press, 2022

12. Madurai Elavarasan R, Nadarajah M, Pugazhendhi R, et al. The untold subtlety of energy consumption and its influence on policy drive towards sustainable development goal 7. Applied Energy, 2023, 334: 120698

13. United Nations General Assembly. Transforming our world: The 2030 agenda for sustainable development. 2023–9–28, available at the website of UN

14. Nundy S, Ghosh A, Mesloub A, et al. Impact of Covid-19 pandemic on socio-economic, energy-environment and transport sector globally and sustainable development goal (SDG). Journal of Cleaner Production, 2021, 312: 127705

15. Liu W, Shen Y, Razzaq A. How renewable energy investment, environmental regulations, and financial development derive renewable energy transition: Evidence from G7 countries. Renewable Energy, 2023, 206: 1188–1197

16. Babayomi O O, Dahoro D A, Zhang Z. Affordable clean energy transition in developing countries: Pathways and technologies. iScience, 2022, 25(5): 104178

17. Sueyoshi T, Mo F, Wang D D. Sustainable development of countries all over the world and the impact of renewable energy. Renewable Energy, 2022, 184: 320–331

18. Cordroch L, Hilpert S, Wiese F. Why renewables and energy efficiency are not enough—The relevance of sufficiency in the heating sector for limiting global warming to 1.5 °C. Technological Forecasting and Social Change, 2022, 175: 121313

19. Chapman A, Shigetomi Y, Ohno H, et al. Evaluating the global impact of low-carbon energy transitions on social equity. Environmental Innovation and Societal Transitions, 2021, 40: 332–347

20. Nakaishi T, Chapman A, Kagawa S. Shedding light on the energy-related social equity of nations toward a just transition. Socio-Economic Planning Sciences, 2022, 83: 101350

21. Tran T T D, Smith A D. Incorporating performance-based global sensitivity and uncertainty analysis into LCOE calculations for emerging renewable energy technologies. Applied Energy, 2018, 216: 157–171

22. Bolinger M, Wiser R, O'Shaughnessy E. Levelized cost-based learning analysis of utility-scale wind and solar in the united states. iScience, 2022, 25(6): 104378

23. Fritts C E. On a new form of selenium cell, and some electrical discoveries made by its use. American Journal of Science, 1883, s3-26(156): 465–472

24. Green M A, Dunlop E D, Siefer G, et al. Solar cell efficiency tables (version 61). Progress in Photovoltaics: Research and Applications, 2023, 31(1): 3–16

25. Garud S, Trinh C T, Abou-Ras D, et al. Toward high solar cell efficiency with low material usage: 15% efficiency with 14 mm polycrystalline silicon on glass. Solar RRL, 2020, 4(6): 2000058

26. Rawat S, Gupta R, Gohri S. Performance assessment of CIGS solar cell with different CIGS grading profile. Materials Today: Proceedings, 2023

27. Bhattarai S, Mhamdi A, Hossain I, et al. A detailed review of perovskite solar cells: Introduction, working principle, modelling, fabrication techniques, future challenges. Micro and Nanostructures, 2022, 172: 207450

28. Hong L, Ge Z. Single-component organic solar cells with over 11% efficiency. Chem, 2021, 7(8): 1987–1989

29. van Zalk J, Behrens P. The spatial extent of renewable and non-renewable power generation: A review and meta-analysis of power densities and their application in the U.S. Energy Policy, 2018, 123: 83–91

30. Fontani D, Jafrancesco D, Sansoni P, et al. Field optimization for bifacial modules. Optical Materials, 2023, 138: 113715

31. Guerrero-Lemus R, Vega R, Kim T, et al. Bifacial solar photovoltaics—A technology review. Renewable & Sustainable Energy Reviews, 2016, 60: 1533–1549

32. Gu W, Ma T, Ahmed S, et al. A comprehensive review and outlook of bifacial photovoltaic (BPV) technology. Energy Conversion and Management, 2020, 223: 113283

33. Lorenzo E. On the historical origins of bifacial PV modelling. Solar Energy, 2021, 218: 587–595

34. Raina G, Sinha S. A holistic review approach of design considerations, modelling, challenges and future applications for bifacial photovoltaics. Energy Conversion and Management, 2022, 271: 116290

35. de Bastiani M, Subbiah A S, Babics M, et al. Bifacial perovskite/silicon tandem solar cells. Joule, 2022, 6(7): 1431–1445

36. Mouhib E, Micheli L, Almonacid F M, et al. Overview of the fundamentals and applications of bifacial photovoltaic technology: Agrivoltaics and aquavoltaics. Energies, 2022, 15(23): 8777

37. Molto C, Oh J, Mahmood F I, et al. Review of potential-induced degradation in bifacial photovoltaic modules. Energy Technology, 2023, 11(4): 2200943

38. Eguren J, Martínez-Moreno F, Merodio P, et al. First bifacial PV modules early 1983. Solar Energy, 2022, 243: 327–335

39. Cuevas A, Luque A, Eguren J, et al. 50 percent more output power from an albedo-collecting flat panel using bifacial. Solar Cells, 1982, 29(5): 419–420

40. Raina G, Sinha S. A comprehensive assessment of electrical performance and mismatch losses in bifacial PV module under different front and rear side shading scenarios. Energy Conversion and Management, 2022, 261: 115668

41. Muehleisen W, Loeschnig J, Feichtner M, et al. Energy yield measurement of an elevated PV system on a white flat roof and a performance comparison of monofacial and bifacial modules. Renewable Energy, 2021, 170: 613–619

42. Khan M R, Hanna A, Sun X, et al. Vertical bifacial solar farms: Physics, design, and global optimization. Applied Energy, 2017, 206: 240–248

43. Guo S, Walsh T M, Peters M. Vertically mounted bifacial photovoltaic modules: A global analysis. Energy, 2013, 61: 447–454

44. Hou Q, Zhang N, Du E, et al. Probabilistic duck curve in high PV penetration power system: Concept, modeling, and empirical analysis in China. Applied Energy, 2019, 242: 205–215

45. Patel M T, Khan M R, Sun X, et al. A worldwide cost-based design and optimization of tilted bifacial solar farms. Applied Energy, 2019, 247: 467–479

46. Appelbaum J. Bifacial photovoltaic panels field. Renewable Energy, 2016, 85: 338–343

47. Khan M R, Sakr E, Sun X, et al. Ground sculpting to enhance energy yield of vertical bifacial solar farms. Applied Energy, 2019, 241: 592–598

48. Perin Gasparin F, Detzel Kipper F, Schuck de Oliveira F, et al. Assessment on the variation of temperature coefficients of photovoltaic modules with solar irradiance. Solar Energy, 2022, 244: 126–133

49. Prasad M, Prasad R. Bifacial vs monofacial grid-connected solar photovoltaic for small islands: A case study of Fiji. Renewable Energy, 2022, 203: 686–702

50. Tahir F, Baloch A A B, Al-Ghamdi S G. Impact of climate change on solar monofacial and bifacial photovoltaics (PV) potential in Qatar. Energy Reports, 2022, 8: 518–522

51. Li J, Zhou Y, Niu X, et al. Performance evaluation of bifacial PV modules using high thermal conductivity fins. Solar Energy, 2022, 245: 108–119

52. Xia T, Chen H, Wang H. Self-protecting concave microstructures on glass surface for daytime radiative cooling in bifacial solar cells. International Communications in Heat and Mass Transfer, 2023, 142: 106666

53. Ma T, Kazemian A, Habibollahzade A, et al. A comparative study on bifacial photovoltaic/thermal modules with various cooling methods. Energy Conversion and Management, 2022, 263: 115555

54. Gao Y, Wang C, Wu D, et al. A numerical evaluation of the bifacial concentrated PV-STEG system cooled by mini-channel heat sink. Renewable Energy, 2022, 192: 716–730

55. Zainali S, Qadir O, Parlak S C, et al. Computational fluid dynamics modelling of microclimate for a vertical agrivoltaic system. Energy Nexus, 2023, 9: 100173

56. Dinesh H, Pearce J M. The potential of agrivoltaic systems. Renewable & Sustainable Energy Reviews, 2016, 54: 299–308

57. Reasoner M, Ghosh A. Agrivoltaic engineering and layout optimization approaches in the transition to renewable energy technologies: A review. Challenges, 2022, 13(2): 43

58. Handler R, Pearce J M. Greener sheep: Life cycle analysis of integrated sheep agrivoltaic systems. Cleaner Energy Systems, 2022, 3: 100036

59. Ramkiran B, Sundarabalan C K, Sudhakar K. Sustainable

passive cooling strategy for PV module: A comparative analysis. Case Studies in Thermal Engineering, 2021, 27: 101317

60. Campana P E, Stridh B, Amaducci S, et al. Optimisation of vertically mounted agrivoltaic systems. Journal of Cleaner Production, 2021, 325: 129091

61. Williams H J, Hashad K, Wang H, et al. The potential for agrivoltaics to enhance solar farm cooling. Applied Energy, 2023, 332: 120478

62. Kreinin L, Bordin N, Karsenty A, et al. PV module power gain due to bifacial design. Preliminary experimental and simulation data. In: 2010 35th IEEE Photovoltaic Specialists Conference, Honolulu, HI, USA, 2010, 002171–002175

63. Ziar H, Sönmez F F, Isabella O, et al. A comprehensive albedo model for solar energy applications: Geometric spectral albedo. Applied Energy, 2019, 255: 113867

64. Zheng L, Zhao G, Dong J, et al. Spatial, temporal, and spectral variations in albedo due to vegetation changes in China's grasslands. ISPRS Journal of Photogrammetry and Remote Sensing, 2019, 152: 1–12

65. Wang R, Chen J M, Pavlic G, et al. Improving winter leaf area index estimation in coniferous forests and its significance in estimating the land surface albedo. ISPRS Journal of Photogrammetry and Remote Sensing, 2016, 119: 32–48

66. Katsikogiannis O A, Ziar H, Isabella O. Integration of bifacial photovoltaics in agrivoltaic systems: A synergistic design approach. Applied Energy, 2022, 309: 118475

67. Marrou H, Guilioni L, Dufour L, et al. Microclimate under agrivoltaic systems: Is crop growth rate affected in the partial shade of solar panels? Agricultural and Forest Meteorology, 2013, 177: 117–132

68. Amaducci S, Yin X, Colauzzi M. Agrivoltaic systems to optimise land use for electric energy production. Applied Energy, 2018, 220: 545–561

69. Deline C, MacAlpine S, Marion B, et al. Assessment of bifacial photovoltaic module power rating methodologies-inside and out. IEEE Journal of Photovoltaics, 2017, 7(2): 575–580

70. Riaz M H, Imran H, Younas R, et al. The optimization of vertical bifacial photovoltaic farms for efficient agrivoltaic systems. Solar Energy, 2021, 230: 1004–1012

71. Ding L, Zhu Y, Zheng L, et al. What is the path of photovoltaic building (BIPV or BAPV) promotion?—The perspective of evolutionary games. Applied Energy, 2023, 340: 121033

72. Peng C, Huang Y, Wu Z. Building-integrated photovoltaics (BIPV) in architectural design in China. Energy and Building, 2011, 43(12): 3592–3598

73. Barkaszi S F, Dunlop J P. Discussion of strategies for mounting photovoltaic arrays on rooftops. In: Solar Engineering 2001—Forum 2001 Solar Energy—The Power to Choose, American Society of Mechanical Engineers, Washington, DC, USA, 2001, 333–338

74. Custódio I, Quevedo T, Melo A P, et al. A holistic approach for assessing architectural integration quality of solar photovoltaic rooftops and shading devices. Solar Energy, 2022, 237: 432–446

75. Liu K, Zhu B, Chen J. Low-carbon design path of building integrated photovoltaics: A comparative study based on green building rating systems. Buildings, 2021, 11(10): 469

76. Ghosh A. Potential of building integrated and attached/applied photovoltaic (BIPV/BAPV) for adaptive less energy-hungry building's skin: A comprehensive review. Journal of Cleaner Production, 2020, 276: 123343

77. Peng C, Huang Y, Wu Z. Building-integrated photovoltaics (BIPV) in architectural design in China. Energy and Building, 2011, 43(12): 3592–3598

78. Mazzeo D, Matera N, Peri G, et al. Forecasting green roofs' potential in improving building thermal performance and mitigating urban heat island in the Mediterranean area: An artificial intelligence-based approach. Applied Thermal Engineering, 2023, 222: 119879

79. Baumann T, Nussbaumer H, Klenk M, et al. Photovoltaic systems with vertically mounted bifacial PV modules in combination with green roofs. Solar Energy, 2019, 190: 139–146

80. Tillmann P, Jäger K, Becker C. Minimising the levelised cost of electricity for bifacial solar panel arrays using Bayesian optimisation. Sustainable Energy & Fuels, 2023(4), 254–264

81. Martin S. What PV installers expect in 2023. 2023–9–28, available at the website of PV-magazine

82. Bretz S E, Akbari H. Long-term performance of high-albedo roof coatings. Energy and Building, 1997, 25(2): 159–167

83. Ramamurthy P, Sun T, Rule K, et al. The joint influence of albedo and insulation on roof performance: An observational study. Energy and Building, 2015, 93: 249–258

84. Del Barrio E P. Analysis of the green roofs cooling potential in buildings. Energy and Building, 1998, 27(2): 179–193

85. Santamouris M. Cooling the cities—A review of reflective and green roof mitigation technologies to fight heat island and improve comfort in urban environments. Solar Energy, 2014, 103: 682–703

86. Xiao B, Bowker M A. Moss-biocrusts strongly decrease soil surface albedo, altering land-surface energy balance in a dryland ecosystem. Science of the Total Environment, 2020, 741: 140425

87. Yang T, Athienitis A K. A review of research and developments of building-integrated photovoltaic/thermal (BIPV/T) systems. Renewable & Sustainable Energy Reviews, 2016, 66: 886–912

88. Ghosh A, Sundaram S, Mallick T K. Investigation of thermal and electrical performances of a combined semi-transparent PV-vacuum glazing. Applied Energy, 2018, 228: 1591–1600

89. Roy A, Ghosh A, Bhandari S, et al. Perovskite solar cells for BIPV application: A review. Buildings, 2020, 10(7): 129

90. Chen M, Zhang W, Xie L, et al. Improvement of the electricity performance of bifacial PV module applied on the building envelope. Energy and Building, 2021, 238: 110849

91. Zhao O, Zhang W, Xie L, et al. Investigation of indoor environment and thermal comfort of building installed with bifacial PV modules. Sustainable Cities and Society, 2022, 76: 113463

92. Akbari Paydar M. Optimum design of building integrated PV module as a movable shading device. Sustainable Cities and Society, 2020, 62: 102368

93. Kang S, Hwang T, Kim J T. Theoretical analysis of the blinds integrated photovoltaic modules. Energy and Building, 2012, 46:

86–91

94. Thebault M, Clivillé V, Berrah L, et al. Multicriteria roof sorting for the integration of photovoltaic systems in urban environments. Sustainable Cities and Society, 2020, 60: 102259

95. Kubota T, Chyee D T H, Ahmad S. The effects of night ventilation technique on indoor thermal environment for residential buildings in hot-humid climate of Malaysia. Energy and Building, 2009, 41(8): 829–839

96. Guo W, Kong L, Chow T, et al. Energy performance of photovoltaic (PV) windows under typical climates of China in terms of transmittance and orientation. Energy, 2020, 213: 118794

97. Roy A, Ghosh A, Bhandari S, et al. Color comfort evaluation of dye-sensitized solar cell (DSSC) based building-integrated photovoltaic (BIPV) glazing after 2 years of ambient exposure. Journal of Physical Chemistry C, 2019, 123(39): 23834–23837

98. Ghosh A. Fenestration integrated BIPV (FIPV): A review. Solar Energy, 2022, 237: 213–230

99. Ghosh A, Sundaram S, Mallick T K. Colour properties and glazing factors evaluation of multicrystalline based semi-transparent photovoltaic-vacuum glazing for BIPV application. Renewable Energy, 2019, 131: 730–736

100. Tina G M, Scavo F B, Aneli S, et al. Assessment of the electrical and thermal performances of building integrated bifacial photovoltaic modules. Journal of Cleaner Production, 2021, 313: 127906

101. Gagliano A, Nocera F, Aneli S. Thermodynamic analysis of ventilated façades under different wind conditions in summer period. Energy and Building, 2016, 122: 131–139

102. Guillén I, Gómez-Lozano V, Fran J M, et al. Thermal behavior analysis of different multilayer façade: Numerical model versus experimental prototype. Energy and Building, 2014, 79: 184–190

103. Ciampi M, Leccese F, Tuoni G. Ventilated facades energy performance in summer cooling of buildings. Solar Energy, 2003, 75(6): 491–502

104. Yoo S H, Lee E T. Efficiency characteristic of building integrated photovoltaics as a shading device. Building and Environment, 2002, 37(6): 615–623

105. Chae Y T, Kim J, Park H, et al. Building energy performance evaluation of building integrated photovoltaic (BIPV) window with semi-transparent solar cells. Applied Energy, 2014, 129: 217–227

106. Alrashidi H, Ghosh A, Issa W, et al. Thermal performance of semitransparent CDTE BIPV window at temperate climate. Solar Energy, 2020, 195: 536–543

107. Assoa Y B, Thony P, Messaoudi P, et al. Study of a building integrated bifacial photovoltaic facade. Solar Energy, 2021, 227: 497–515

108. Tina G M, Bontempo Scavo F, Merlo L, et al. Comparative analysis of monofacial and bifacial photovoltaic modules for floating power plants. Applied Energy, 2021, 281: 116084

109. Ghosh A. A comprehensive review of water based PV: Flotavoltaics, under water, offshore & canal top. Ocean Engineering, 2023, 281: 115044

110. El Hammoumi A, Chtita S, Motahhir S, et al. Solar PV energy:

From material to use, and the most commonly used techniques to maximize the power output of PV systems: A focus on solar trackers and floating solar panels. Energy Reports, 2022, 8: 11992–12010

111. Essak L, Ghosh A. Floating photovoltaics: A review. Cleanroom Technology, 2022, 4(3): 752–769

112. Nisar H, Janjua A K, Hafeez H, et al. Thermal and electrical performance of solar floating PV system compared to on-ground PV system—An experimental investigation. Solar Energy, 2022, 241: 231–247

113. Rosa-Clot M, Tina G M, Nizetic S. Floating photovoltaic plants and wastewater basins: An Australian project. Energy Procedia, 2017, 134: 664–674

114. Sacramento E M, Carvalho P C M, de Araújo J C, et al. Scenarios for use of floating photovoltaic plants in Brazilian reservoirs. IET Renewable Power Generation, 2015, 9(8): 1019–1024

115. Cazzaniga R, Rosa-Clot M. The booming of floating PV. Solar Energy, 2021, 219: 3–10

116. Rosa-Clot M, Tina G M. Submerged and Floating Photovoltaic Systems: Modelling, Design and Case Studies. London: Elsevier, 2018

117. Kakoulaki G, Gonzalez Sanchez R, Gracia Amillo A, et al. Benefits of pairing floating solar photovoltaics with hydropower reservoirs in Europe. Renewable & Sustainable Energy Reviews, 2023, 171: 112989

118. Silvério N M, Barros R M, Tiago Filho G L, et al. Use of floating PV plants for coordinated operation with hydropower plants: Case study of the hydroelectric plants of the São Francisco river basin. Energy Conversion and Management, 2018, 171: 339–349

119. Ji Q, Li K, Wang Y, et al. Effect of floating photovoltaic system on water temperature of deep reservoir and assessment of its potential benefits, a case on Xiangjiaba reservoir with hydropower station. Renewable Energy, 2022, 195: 946–956

120. Cogley J G. The albedo of water as a function of latitude. Monthly Weather Review, 1979, 107(6): 775–781

121. Du J, Zhou H, Jacinthe P A, et al. Retrieval of lake water surface albedo from Sentinel-2 remote sensing imagery. Journal of Hydrology, 2023, 617: 128904

122. Hasan A, Dincer I. A new performance assessment methodology of bifacial photovoltaic solar panels for offshore applications. Energy Conversion and Management, 2020, 220: 112972

123. Cuce E, Cuce P M, Saboor S, et al. Floating PVs in terms of power generation, environmental aspects, market potential, and challenges. Sustainability, 2022, 14(5): 2626

124. Hutchins M. Investigating bifacial for floating PV. 2023–9-28, available at PV-magazine

125. Enaganti P K, Bhattacharjee A, Ghosh A, et al. Experimental investigations for dust build-up on low-iron glass exterior and its effects on the performance of solar PV systems. Energy, 2022, 239: 122213

126. Chanchangi Y N, Ghosh A, Sundaram S, et al. Dust and PV performance in Nigeria: A review. Renewable & Sustainable Energy Reviews, 2020, 121: 109704

127. Ghosh A. Soiling losses: A barrier for India's energy security

dependency from photovoltaic power. Challenges, 2020, 11(1): 9

128. Kumar Yadav S, Manoj Kumar N, Ghosh A, et al. Assessment of soiling impacts and cleaning frequencies of a rooftop BAPV system in composite climates of India. Solar Energy, 2022, 242: 119–129

129. Untila G G, Kost T N, Chebotareva A B, et al. Bifacial concentrator Ag-free crystalline n-type Si solar cell. Progress in Photovoltaics: Research and Applications, 2015, 23(5): 600–610

130. Ohtsuka H, Sakamoto M, Koyama M, et al. Characteristics of bifacial solar cells under bifacial illumination with various intensity levels. Progress in Photovoltaics: Research and Applications, 2001, 9(1): 1–13

131. Singh J P, Walsh T M, Aberle A G. A new method to characterize bifacial solar cells. Progress in Photovoltaics: Research and Applications, 2014, 22(8): 903–909

132. Alam M, Gul M S, Muneer T. Performance analysis and comparison between bifacial and monofacial solar photovoltaic at various ground albedo conditions. Renewable Energy Focus, 2023, 44: 295–316

133. Iqbal M. An Introduction to Solar Radiation. London: Elsevier, 1983

134. Rodríguez-Gallegos C D, Bieri M, Gandhi O, et al. Monofacial vs bifacial Si-based PV modules: Which one is more cost-effective? Solar Energy, 2018, 176: 412–438

135. Martin N, Ruiz J M. Calculation of the PV modules angular losses under field conditions by means of an analytical model. Solar Energy Materials and Solar Cells, 2001, 70(1): 25–38

136. Martín N, Ruiz J M. Annual angular reflection losses in PV modules. Progress in Photovoltaics: Research and Applications, 2005, 13(1): 75–84

137. Gueymard C A. Direct and indirect uncertainties in the prediction of tilted irradiance for solar engineering applications. Solar Energy, 2009, 83(3): 432–444

138. Yang D. Solar radiation on inclined surfaces: Corrections and benchmarks. Solar Energy, 2016, 136: 288–302

139. Perez R, Stewart R, Arbogast C, et al. An anisotropic hourly diffuse radiation model for sloping surfaces: Description, performance validation, site dependency evaluation. Solar Energy, 1986, 36(6): 481–497

140. Perez R, Seals R, Ineichen P, et al. A new simplified version of the Perez diffuse irradiance model for tilted surfaces. Solar Energy, 1987, 39(3): 221–231

141. Perez R, Stewart R, Seals R, et al. The development and verification of the Perez diffuse radiation model. US Technical Report SAND88-7030, 1988

142. Perez R, Ineichen P, Seals R, et al. Modeling daylight availability and irradiance components from direct and global irradiance. Solar Energy, 1990, 44(5): 271–289

143. Marion B. Numerical method for angle-of-incidence correction factors for diffuse radiation incident photovoltaic modules. Solar Energy, 2017, 147: 344–348

144. Marion B, MacAlpine S, Deline C, et al. A practical irradiance model for bifacial PV modules. In: 2017 IEEE 44th Photovoltaic Specialist Conference, Washington, DC, USA, 2017, 1537–1542

145. Shoukry I, Libal J, Kopecek R, et al. Modelling of bifacial gain for stand-alone and in-field installed bifacial PV modules. Energy Procedia, 2016, 92: 600–608

146. Yusufoglu U A, Pletzer T M, Koduvelikulathu L J, et al. Analysis of the annual performance of bifacial modules and optimization methods. IEEE Journal of Photovoltaics, 2015, 5(1): 320–328

147. Durusoy B, Ozden T, Akinoglu B G. Solar irradiation on the rear surface of bifacial solar modules: A modeling approach. Scientific Reports, 2020, 10(1): 13300

148. Sun B, Lu L, Yuan Y, et al. Development and validation of a concise and anisotropic irradiance model for bifacial photovoltaic modules. Renewable Energy, 2023, 209: 442–452

149. Zhou M, Chen G, Dong Z, et al. Estimation of surface albedo from meteorological observations across China. Agricultural and Forest Meteorology, 2020, 281: 107848

150. Bradley A, Thornes J, Chapman L, et al. Modeling spatial and temporal road thermal climatology in rural and urban areas using a GIS. Climate Research, 2002, 22: 41–55

151. Taha H, Sailor D, Akbari H. High-albedo materials for reducing building cooling energy use. US Technical Report LBL-31721, 1992

152. Rosenberg N J, Blad B L, Verma S B. Biology and environment, Microclimate, 1983

153. Radionov V, Bryazgin N, Alexandrov E. The snow cover of the arctic basin. US Technical Report APL-UW TR, 9701, 1997

154. Laudani A, Riganti Fulginei F, Salvini A, et al. One diode circuital model of light soaking phenomena in DYE-sensitized solar cells. Optik, 2018, 156: 311–317

155. Raina G, Sinha S. A comprehensive assessment of electrical performance and mismatch losses in bifacial PV module under different front and rear side shading scenarios. Energy Conversion and Management, 2022, 261: 115668

156. Lopez-Garcia J, Casado A, Sample T. Electrical performance of bifacial silicon PV modules under different indoor mounting configurations affecting the rear reflected irradiance. Solar Energy, 2019, 177: 471–482

157. Skoplaki E, Palyvos J A. On the temperature dependence of photovoltaic module electrical performance: A review of efficiency/power correlations. Solar Energy, 2009, 83(5): 614–624

158. Kratochvil J, Boyson W, King D. Photovoltaic array performance model. Sandia National Laboratories Technical Report SAND2004–3535, 2004

159. Fanney A, Davis M, Dougherty B. Short-term characterization of building integrated photovoltaic panel. Journal of Solar Energy Engineering, 2003, 125(1): 13–20

160. King D L, Kratochvil J A, Boyson W E. Measuring solar spectral and angle-of-incidence effects on photovoltaic modules and solar irradiance sensors. In: Conference Record of the 26th IEEE Photovoltaic Specialists Conference, Anaheim, CA, USA, 1997

161. Kasten F, Young A T. Revised optical air mass tables and approximation formula. Applied Optics, 1989, 28(22): 4735–4738

162. Arno S, Klaus J, Olindo I, et al. Solar Energy: The Physics and Engineering of Photovoltaic Conversion, Technologies and

Systems. Cambridge: UIT, 2016

163. Mannino G, Tina G M, Cacciato M, et al. A photovoltaic degradation evaluation method applied to bifacial modules. Solar Energy, 2023, 251: 39–50

164. Kim J, Rabelo M, Padi S P, et al. A review of the degradation of photovoltaic modules for life expectancy. Energies, 2021, 14(14): 4278

165. Theristis M, Stein J S, Deline C, et al. Onymous early-life performance degradation analysis of recent photovoltaic module technologies. Progress in Photovoltaics: Research and Applications, 2023, 31(2): 149–160

166. da Silva M K, Gul M S, Chaudhry H. Review on the sources of power loss in monofacial and bifacial photovoltaic technologies. Energies, 2021, 14(23): 7935

167. Hutchins M. Filling in the (micro)cracks. 2023–9–28, available at the website of PV-magazine

168. Guo B, Javed W, Khoo Y S, et al. Solar PV soiling mitigation by electrodynamic dust shield in field conditions. Solar Energy, 2019, 188: 271–277

169. Ratnaparkhi A, Dave D, Valerino M, et al. Reduction in solar PV soiling loss using hydrophobic coating with and without dew suppression. Solar Energy, 2023, 253: 332–342

170. Rodríguez-Gallegos C D, Liu H, Gandhi O, et al. Global techno-economic performance of bifacial and tracking photovoltaic systems. Joule, 2020, 4(7): 1514–1541

171. Papapetrou M, Kosmadakis G. Chapter 9—Resource, environmental, and economic aspects of SGHE. In: Tamburini A, Cipollina A, Micale G, eds. Salinity Gradient Heat Engines. Cambridge: Woodhead Publishing, 2022, 319–353

172. Rodríguez-Gallegos C D, Gandhi O, Bieri M, et al. A diesel replacement strategy for off-grid systems based on progressive introduction of PV and batteries: An Indonesian case study. Applied Energy, 2018, 229: 1218–1232

173. Rodríguez-Gallegos C D, Yang D, Gandhi O, et al. A multi-objective and robust optimization approach for sizing and placement of PV and batteries in off-grid systems fully operated by diesel generators: An Indonesian case study. Energy, 2018, 160: 410–429

174. Chang R, Cao Y, Lu Y, et al. Should BIPV technologies be empowered by innovation policy mix to facilitate energy transitions?—Revealing stakeholders' different perspectives using Q methodology. Energy Policy, 2019, 129: 307–318

175. Rogge K S, Schleich J. Do policy mix characteristics matter for low-carbon innovation? A survey-based exploration of renewable power generation technologies in Germany. Research Policy, 2018, 47(9): 1639–1654

176. Shubbak M H. The technological system of production and innovation: The case of photovoltaic technology in China. Research Policy, 2019, 48(4): 993–1015

177. Che X J, Zhou P, Chai K H. Regional policy effect on photovoltaic (PV) technology innovation: Findings from 260 cities in China. Energy Policy, 2022, 162: 112807

178. Gao X, Rai V. Local demand-pull policy and energy innovation: Evidence from the solar photovoltaic market in China. Energy Policy, 2019, 128: 364–376

179. Lin B, Luan R. Do government subsidies promote efficiency in technological innovation of China's photovoltaic enterprises? Journal of Cleaner Production, 2020, 254: 120108

180. Costantini V, Crespi F, Martini C, et al. Demand-pull and technology-push public support for eco-innovation: The case of the biofuels sector. Research Policy, 2015, 44(3): 577–595

181. Johnstone N, Haščič I, Popp D. Renewable energy policies and technological innovation: Evidence based on patent counts. Environmental and Resource Economics, 2010, 45(1): 133–155

182. Ra N, Ghosh A, Bhattacharjee A. IoT-based smart energy management for solar vanadium redox flow battery powered switchable building glazing satisfying the HVAC system of EV charging stations. Energy Conversion and Management, 2023, 281: 116851

183. Ghosh A. Possibilities and challenges for the inclusion of the electric vehicle (EV) to reduce the carbon footprint in the transport sector: A review. Energies, 2020, 13(10): 2602

184. Bhattacharjee A, Samanta H, Ghosh A, et al. Optimized integration of hybrid renewable sources with long-life battery energy storage in microgrids for peak power shaving and demand side management under different tariff scenario. Energy Technology, 2021, 9(9): 2100199

185. Khan S, Sudhakar K, bin Yusof M H. Comparison of mono and bifacial modules for building integration and electric vehicle charging: A case study in Sweden. Energy Conversion and Management, 2023, 20: 100420